Published in final edited form as:
J Immunol. 2012 December 15; 189(12): 5667–5681. doi:10.4049/jimmunol.1201661.

The lupus-prone NZM2410/NZW strain derived *Sle1b* sub-locus alters the germinal center checkpoint in female mice in a B cell intrinsic manner

Eric B. Wong[*,†], **Tahsin N. Khan**[*,†], **Chandra Mohan**[‡], and **Ziaur S.M. Rahman**[*,†]

[*]Department of Microbiology and Immunology, Jefferson Medical College, Jefferson Alumni Hall, Room 461, 1020 Locust Street, Philadelphia, PA 19107

[‡]Division of Rheumatology, Department of Internal Medicine, University of Texas Southwestern Medical Center, Dallas, TX 75390

Abstract

C57BL/6 (B6) mice carrying the *Sle1b* sub-locus (named B6.*Sle1b*), which harbors the lupus-associated NZM2410/NZW SLAM family genes, produce anti-nuclear antibodies (ANA). However, the role and mechanism(s) involved in the alteration of the germinal center (GC) tolerance checkpoint in the development of ANAs in these mice is not defined. Here we show significantly higher spontaneously formed GCs (Spt-GCs) in B6.*Sle1b* female mice compared to B6 controls. We also found a significant increase in $CD4^{+}CXCR5^{hi}PD\text{-}1^{hi}$ spontaneously activated follicular helper T (Spt-T_{FH}) cells in B6.*Sle1b* female mice. Compared to B6 controls, B6.*Sle1b* female mice had increased numbers of proliferating B cells predominantly located in Spt-GCs. The elevated Spt-GCs in B6.*Sle1b* female mice were strongly associated with increased ANA-specific antibody forming cells (AFCs) and ANA titers. The increased numbers of Spt-GCs and Spt-T_{FH} cells in B6.*Sle1b* mice were not the result of a generalized defect in B cells expressing *Sle1b*. Consistent with the elevated spontaneous response in B6.*Sle1b* mice, the attenuated GC response characteristic of DNA and p-azophenylarsonate (Ars) reactive B cells from Ig V_H knock-in mice (termed HKIR) were relieved in adoptively transferred recipients in the presence of *Sle1b*. Finally, by generating mixed bone marrow chimeras, we showed that the effect of *Sle1b* on Spt-GC, T_{FH} cell and autoantibody responses in B6.*Sle1b* mice was B cell autonomous. These data indicate that the NZM2410/NZW-derived *Sle1b* sub-locus in conjunction with the female sex primarily affects B cells leading to the alteration of the GC tolerance checkpoint and the generation of ANA-specific AFCs.

Keywords

Rodent; B cells; autoimmunity; Systemic Lupus Erythematosus; antibody forming cell response; germinal center response

Introduction

The lupus-prone New Zealand Black/New Zealand White (NZB/NZW)-derived NZM2410 mouse strain develops a disease phenotype that closely resembles human SLE (systemic

[2]Address correspondence and reprint requests to Dr. Ziaur Rahman, Department of Microbiology and Immunology, H107, Pennsylvania State University College of Medicine, 500 University Drive, Hershey, PA 17033-0850. zrahman@hmc.psu.edu.
[†]Current address: Department of Microbiology and Immunology, Pennsylvania State University College of Medicine, Hershey, PA17033.

lupus erythematosus). Three major genomic intervals (*Sle1, Sle2, and Sle3*) are responsible for systemic autoimmune disease susceptibility in NZM2410 mice (1–3). B6 mice congenic for the *Sle1* locus develop high titers of IgG autoantibodies against chromatin (4) and generate T cells specific for histone (5), implicating *Sle1* in the loss of tolerance which leads to the development of anti-nuclear antibodies (ANAs). Genetic recombination of the *Sle1* locus has further dissected the locus into four sub-loci termed *Sle1a, Sle1FcR, Sle1b*, and *Sle1c* (6, 7). B6 mice congenic for each sub-locus display partial autoimmune phenotypes with B6.*Sle1b* mice exhibiting gender-biased and highly penetrant ANA production (6). *Sle1b* results in altered functions in both T and B cells (5, 7–9). Resting B cells from B6.*Sle1b* mice appear to be more readily activated and have an enhanced ability to present antigen compared to B cells from B6 mice (10). T cells from B6.*Sle1b* exhibit higher Ca^{+2} flux response after TCR stimulation (7). In addition, a larger percentage of $CD4^+$ T cells from B6.*Sle1b* are $CD69^+CD62L^{lo}CD44^{hi}$ (9). Further confirmation of the importance of the *Sle1b* sub-locus in SLE pathology is evident in B6.*Sle1b* mice which also have either the Y-linked autoimmune accelerator (*yaa*) or lymphoproliferation (*lpr*) gene mutation, as they develop fatal lupus nephritis (11–13).

The *Sle1b* sub-locus contains the SLAM (signaling lymphocyte activation molecule) family (*Slamf*) genes derived from the lupus-prone NZW mice (7). The SLAMF cell surface receptors play an important role in regulating cellular and humoral immunity (14–16). Extensive polymorphisms in the *Slamf* genes have been demonstrated to be responsible for the loss of tolerance to nuclear antigens and for the induction of an autoimmune phenotype in B6.*Sle1b* mice (7). The *Ly108.1* isoform of *Ly108/Slamf6* expressed in B6.*Sle1b* mice is thought to be one of the strongest mediators involved in the loss of early B cell tolerance while *Ly108.2* expression in B6 is believed to play role in the maintenance of tolerance (8). Other studies have implicated the protective role of *CD48/Slamf2* as ablation of *CD48* renders B6.*Sle1b* mice susceptible to the development of lupus-like autoimmune disease (17). While several candidate genes in the SLAM family in B6.*Sle1b* mice may contribute to the loss of tolerance resulting in autoimmune pathology, epistatic interactions between these genes most likely mediate the severity of SLE in these mice.

B cell tolerance to self-Ags (i.e., nuclear-Ags) is maintained through multiple tolerance checkpoints operative centrally in the bone marrow or peripherally in the secondary lymphoid organs (i.e., germinal center (GC) checkpoint). B cells undergo proliferation and somatic hypermutation in GCs, which results in B cells with high and low foreign Ag reactivity and potential autoreactivity. According to the current models of B cell selection in GCs, only high-affinity B cells receive survival signals and are then positively selected for further development into class-switched, high-affinity memory B cells and long-lived antibody forming cells (AFC) (18–20). B cells with low Ag-affinity and/or autoreactivity die via apoptosis (negative selection) (21–23). Altered regulation of positive and negative selection in the GCs in the presence of lupus-associated genes (i.e., lupus alleles of SLAM family genes) may allow autoreactive B cells to escape the GC checkpoint which may lead to the development of autoantibody-producing memory B cells and long-lived AFCs. Strains of mice that develop SLE-like disease spontaneously form GCs in the spleen by 1–2 months of age (24). Autoantibodies detected in lupus patients and lupus-prone mice bind their self-Ag with high affinity, are somatically mutated and class-switched (25–31), thus suggesting a role for the GC pathway in autoantibody production. However, the role and mechanism(s) involved in the alteration of the GC checkpoint in autoantibody production in B6.*Sle1b* mice is unclear.

Follicular helper T cells (T_{FH}) are a subset of $CD4^+$ T cells specialized to aid GC B cell development through B-T co-stimulatory molecule interactions, which include CD40 ligand, ICOS, PD-1 and SLAM. While a break in peripheral B cell tolerance at the GC checkpoint

may allow autoreactive B cells to escape negative selection and enter circulation, T_{FH} cells have also been shown to play a key role in contributing to the development of autoimmunity (32–35). *Sanroque* mice, which have a mutation in the *Roquin (Rc3h1)* gene, spontaneously develop GCs in the spleen and lymph nodes and have significantly increased numbers of activated memory T cells (33, 36). These mice develop an autoimmune profile resembling that of human SLE, coincident with increased T_{FH} cell numbers per GC and development of anti-DNA-specific antibodies (33). Mice having the *yaa* mutation on BXSB background (BXSB.*yaa*) also develop severe autoimmune disease and have increased T_{FH} cell numbers (34, 37). These data indicate the critical role of T_{FH} cells in contributing to autoimmune pathology in several SLE mouse models. However, the role of T_{FH} cells in the formation of Spt-GCs and ANA production in B6.*Sle1b* mice is not clear.

In the present study, we performed a detailed analysis of the impact of the *Sle1b* sub-locus on the loss of tolerance to nuclear antigens with an emphasis on the role in the GC pathway. We studied the formation of spontaneous GCs (Spt-GCs) in B6 and B6.*Sle1b* mice without any immunization, housing them in a pathogen-free barrier facility up to 9 months. B6.*Sle1b* female mice exhibited significantly increased percentages of splenic Spt-GCs and spontaneously activated $CD4^+$ helper T cells including follicular helper T (named Spt-T_{FH}) cells compared to age and sex-matched B6 controls. These elevated percentages of Spt-GCs and Spt-T_{FH} cells in B6.*Sle1b* female mice were strongly correlated with increased numbers of ds-DNA, histone, and nucleosome-specific AFCs of both IgM and IgG isotypes. These mice also exhibited high titers of serum ANA-specific IgG2 Abs. These data suggest that the peripheral tolerance checkpoint that controls the formation of Spt-GCs and Spt-T_{FH} cell numbers is altered by the presence of *Sle1b*. This effect is significant in female, but not in male mice, indicating a role for gender on *Sle1b*-mediated alteration of the peripheral tolerance checkpoint which allows for the development of autoantibody producing long-lived AFCs.

To further study the nature of self-Ags and to determine B cell autonomous effect of *Sle1b* on the alteration of the GC checkpoint, we have used an Ig V_H chain knock-in mouse line termed HKIR (38, 39) that develops B cells reactive to the hapten *p*-azophenyl arsonate (Ars) and also have high avidity for DNA and chromatin-based self-antigens. Because of their dual-reactivity with Ars, HKIR self-reactive B cells can be mobilized into the GC reaction (40, 41) where they can participate but due to their autoreactivity these cells are negatively regulated as characterized by the reduced anti-Ars GC response of DNA-Ars dual-reactive HKIR B cells compared to control B cells that are only reactive to Ars (40–42). Thus, this model allowed us to study the influence of *Sle1b* on the regulation of HKIR DNA-reactive B cells at the GC checkpoint. Using this system we also showed that reduced anti-Ars GC response characteristic of DNA-Ars dual-reactive HKIR B cells was reversed in the presence of *Sle1b*, consistent with the data generated through spontaneous model showing alteration of the GC checkpoint by *Sle1b*. Our bone marrow chimeric experiments further revealed that the alteration of the GC checkpoint by *Sle1b* was B cell intrinsic and the effect of *Sle1b* on T cells appeared to be mediated by B cell defect caused by this sub-locus.

Materials and Methods

Mice

C57BL/6 (B6), B6.μMT and B6.TCRβδ$^{-/-}$ mice were purchased from The Jackson Laboratory and then bred in-house. B6 mice congenic for the *Sle1b* sub-locus (named B6.*Sle1b* mice) (6, 11) and the Ig V_H knock-in mouse line HKIR were described previously (38, 43). The HKIR mice were crossed to B6.*Sle1b* to generate HKIR$^{+/-}$.*Sle1b*$^{+/-}$ (named HKIR.*Sle1b*) mice. All mice were maintained in a pathogen-free barrier facility and were

given only autoclaved food and water. Two to three and six to nine month old B6 and B6.*Sle1b* mice were used in experiments for studying spontaneous B and T cell activation in these mice. The mice designated for use in the sheep red blood cell (SRBC) response experiments were 5 to 6 weeks old when used. All experimental procedures performed on these animals were conducted according to the guidelines of our Institutional Animal Care and Use Committee.

SRBC immunization

Five to six week old B6 and B6.*Sle1b* mice were immunized (i.p) with 200 μl of 10% SRBC (Lampire, Pipersville, PA) in 1XPBS. Mouse spleens were harvested 12 days post immunization for flow cytometric and immunohistological analyses. Serum samples were also collected from these mice prior to sacrifice to measure Ab titers.

Reagents and antibodies for flow cytometry and immunohistology analysis

The following antibodies were utilized for flow cytometric analysis of mouse splenocytes: V500-anti-B220 (RA3-6B2); PeCy7-anti-CD95 (FAS, Jo2); Alexa Fluor 700-anti-CD4 (RM4-5); FITC-Foxp3 (FJK-16s); PE-anti-PD-1 (J43); APC-Cy7- anti-CD25 (PC61); biotin-anti-CXCR5 (2G8); V450-anti-Bcl-6 (K112-91) from BD Pharmingen, San Diego, CA. PerCP-Cy5.5-anti-CD69 (H1.253); PE-Cy5-anti-CD86 (GL1); APC-anti-CD44 (IM7); PE-Cy5-streptavidin (SA) from eBioscience, San Diego, CA. PE-Cy7-anti-CD62L (MEL-14); PE-anti-CD80 (16-10A1) from Biolegend, San Diego, CA. FITC-peanut-agglutinin (PNA) from Sigma-Aldrich, St. Louis, MO.

The follow antibodies were utilized for immunohistochemical analysis of the mouse spleen sections: Biotin-mouse anti-rat IgG (Jackson Immunoresearch Laboratories, West Grove, PA); Alkaline phosphatase (AP)-streptavidin; AP Blue substrate kit III; Vector NovaRED substrate kit (Vector Laboratories, Burlingame, CA); Purified rat anti-mouse Ki67 (ImmunoKontact, Abingdon, UK); FITC-PNA (Sigma-Aldrich, St. Louis, MO). Biotin-MOMA-1 (Abcam, Cambridge, MA); Biotin-anti-IgD (11–26, Southern Biotechnology Associates); PE-Anti-CD4 (GK1.5); FITC-GL7 (RA3-6B2) from BD Pharmingen; PE-Anti-PD-1 (J43), streptavidin Alexa Fluor 633 (Molecular Probes); PE-anti-CD138; Biotin-Anti-BrdU (Bu20a) from Biolegend, San Diego, CA; Purified anti-Foxp3 (FJK-16s; ebioscience, San Diego, CA) and a biotinylated form of the anti-idiotypic mAb E4 (prepared in-house); rabbit anti-mouse Bcl-6 (clone N-3, Santa Cruz Biotechnology, Santa Cruz, CA).

Adoptive transfer

B6 × B6.*Sle1b* F1 (B6.*Sle1b*$^{+/-}$) recipient mice were immunized (i.p.) with 100 μg of Ars-KLH (in alum) 1 week prior to transfer (via retro-orbital i.v.) of MACS-purified 2 × 10^6 splenic B cells from either HKIR or HKIR mice expressing *Sle1b* (HKIR.*Sle1b*) donor mice. These chimeric mice were then injected i.p. with 50 μg of Ars-KLH in PBS immediately after cell transfer. Spleens from the recipient mice were harvested 5 days later and utilized for flow cytometric and immunohistological analysis.

Generation of bone marrow chimeric mice

Ten to twelve week old female B6.μMT (μMT) and B6.TCRβδ-deficient (TCRβδ$^{-/-}$) mice were lethally irradiated with 10.5 gray of γ-radiation prior to transfer via retro-orbital i.v. injection of 7.5 to 10×10^6 T cell-depleted mixed bone marrow cells isolated from 8–10 week old female donor mice (i.e., B6, B6.*Sle1b,* μMT and TCRβδ$^{-/-}$). μMT recipients received either a 1:1 ratio of B6 and μMT or B6.*Sle1b* and μMT bone marrow cells. TCRβδ$^{-/-}$ recipients received either a 1:1 ratio of B6 and TCRβδ$^{-/-}$ or B6.*Sle1b* and TCRβδ$^{-/-}$ bone

marrow cells. The recipient chimeric mice were aged for 6 months post transfer of bone marrow cells.

Flow cytometry

Multi-color flow cytometric analysis was done using multiple combinations of the Abs listed above on cell suspensions prepared from spleens of 6–9 month old and SRBC-immunized B6 and B6.*Sle1b* mice, as well as from recipient B6.*Sle1b*$^{+/-}$ mice adoptively transferred with either HKIR or HKIR.*Sle1b* B cells. Biotinylated Abs were detected with streptavidin-conjugated fluorochromes. Stained cells were analyzed using the BD LSRII flow cytometer. Data were analyzed using FlowJo software (Treestar, San Carlos, CA). Intracellular staining for Foxp3 and Bcl-6 was performed through the use of the Foxp3 intracellular staining kit (eBioscience, San Diego, CA) following manufacturer's directions.

Immunohistology

Spleen cryostat sections (5–6 μm) were prepared as described previously (44). Immunohistology was performed using the Abs listed above and the stained sections were analyzed using a fluorescence microscope (Leica Microsystems) and images were captured as previously described (45).

BrdU cell proliferation experiments

Unimmunized 6–9 month old and SRBC-immunized 5–6 week old B6 and B6.*Sle1b* mice were injected with BrdU (i.p., 0.6 mg per mouse, BD Bioscience, San Diego, CA) 12 hours and 1–2 hours prior to sacrifice. Immunohistological analysis of spleen sections for BrdU^{+} cells was performed using BrdU *in situ* staining kit (BD bioscience, San Diego, CA) following manufacturer's guidelines.

ELISpot assays

ELISpot assays were performed as described (42). Briefly, splenocyte suspensions from 6–9 month old B6 and B6.*Sle1b* mice were plated at either 1×10^5 cells/well in IgM and IgG coated or at 1×10^6 cells/well in double-stranded DNA-, histone-, and nucleosome-coated multiscreen 96-well filtration plates (Millipore, Bedford, MA), diluted serially (1:2) and incubated for 6 hr at 37°C. Splenocytes from SRBC-immunized mice were plated at 1×10^6 cells/well. IgM-producing AFCs were detected using biotinylated anti-mouse IgM (Jackson Immunoresearch, West Grove, PA) and streptavidin (SA)-alkaline phosphatase (Vector Laboratories, Burlingame, CA). IgG-producing AFCs were detected using alkaline-phosphatase conjugated anti-mouse IgG (Molecular Probes, Grand Island, NY). Double-stranded DNA-, histone-, and nucleosome-specific AFCs were detected by biotinylated anti-kappa Ab (Invitrogen, Grand Island, NY) and streptavidin (SA)-alkaline phosphatase (Vector Laboratories, Burlingame, CA). Plates were developed using the Vector Blue Alkaline-phosphatase Substrate Kit III (Vector Laboratories, Burlingame, CA). ELISpots were counted using a computerized imaging video system (Cellular Technology, Cleveland, OH).

ANA titers

Total serum ANA titers from 6–9 month old B6 and B6.*Sle1b* mice were measured in ELISA plates coated with either double-stranded DNA, histone, or nucleosome and detected with biotinylated anti-kappa Ab (Invitrogen, Grand Island, NY). Similarly, IgG subtype-specific ANA titers were measured by biotinylated-IgG1, biotinylated IgG2b, and AP-IgG2c (Southern Biotech, Birmingham, AL). Biotinylated antibodies were detected by streptavidin (SA)-alkaline phosphatase (Vector Laboratories, Burlingame, CA). The plates were developed by the PNPP (*p*-Nitrophenyl Phosphate, Disodium Salt) (Thermo Fisher

Scientific, Rockford, IL) substrates for alkaline phosphatase. Serum samples were first diluted in PBS and then subsequently two-fold serial dilution was carried out for each sample. The dilution factor for each sample was generated in a logarithmic scale via the software named "Origin" based on the different OD values of 0.8, 0.9 or 1.0 (at 405 nm) set for different isotype-specific ELISA. The OD values of 0.8, 0.9 or 1.0 were determined based on the linear distribution of most of the samples in any given ELISA. In this way, a dilution factor of 400 for a particular sample with an OD value of 1.0 would indicate that this particular serum sample needed to be diluted 400 times to obtain an OD value of 1.0 at 405 nm. In contrast, a serum sample with a dilution factor of 150 needed to be diluted 150 times to obtain the same OD value. Therefore, the higher the dilution factor in an individual mouse the higher the Ab titers for that particular animal.

Statistical analysis

Statistical analysis was done using Student's *t*-test. P values of <0.05, <0.01, and <0.001 are depicted as *, **, and *** respectively. Statistical significance for the correlation graphs was performed by using regression (R)/ANOVA (analysis of variance).

Results

Effects of Sle1b and gender on spontaneous activation of B cells and CD4 helper T cells

Previous studies have indicated the influence of *Sle1b* sub-locus carrying NZM2410/NZW lupus alleles of the SLAM family genes on both B cells and CD4 helper T cells (9, 11, 13). However, the effects of gender on the spontaneous activation of B and T cells in B6.*Sle1b* mice are not defined. Here we performed a detailed analysis of the influence of *Sle1b* and gender on B cells and CD4 T cells by analyzing both male and female mice. Splenocytes obtained from 6–9 month old B6 and B6.*Sle1b* mice were stained with antibodies against B cell activation markers CD69, CD80 and CD86. The percentage of $B220^{+}CD69^{+}$ (rectangular gates and scatter plot, Fig. 1A) and $B220^{+}CD86^{+}$ (Fig. 1B) B cells were significantly higher in B6.*Sle1b* female mice compared to B6.*Sle1b* males, B6 males and B6 females. In B6 mice, while the percentage of $B220^{+}CD69^{+}$ cells was similar between the two sexes, females had elevated $B220^{+}CD86^{+}$ cells compared to males (Fig. 1A and B). We found no difference in the percentage of $B220^{+}CD80^{+}$ B cells among the four groups of mice (data not shown).

Similar flow cytometric analysis of $CD4^{+}$ T cells using T cell markers, CD4, CD44, CD62L and CD69 revealed significantly higher percentages of both $CD4^{+}CD44^{hi}CD62L^{lo}$ short-lived effector (Fig. 1C, middle panel) and $CD4^{+}CD44^{hi}CD62L^{hi}$ effector memory (Fig. 1C, right panel) helper T cells in splenocytes from B6.*Sle1b* males compared to B6 males. $CD4^{+}CD44^{hi}CD62L^{hi}$ effector memory T cells appeared to be significantly increased in B6.*Sle1b* females compared to B6 females (Fig. 1C, right panel). Both these effector populations were significantly higher in B6 females compared to males (Fig. 1C). We also observed that the percentage of $CD4^{+}CD69^{+}$ cells in B6.*Sle1b* mice (males and females) was significantly increased compared to their B6 control counterparts (rectangular gates and scatter plot, Fig. 1D). These differences were also observed between males and females of each genotype (Fig. 1D).

Significantly higher spontaneously formed GCs (Spt-GCs) in B6.Sle1b mice

GCs are spontaneously formed (named Spt-GC) in lupus-prone mice (24) and human SLE patients (46, 47). Given the increased percentage of activated B cells in 6–9 month old B6.*Sle1b* mice, we examined whether GCs were spontaneously formed in the presence of *Sle1b*. Flow cytometric analysis was performed on splenocytes obtained from B6 and B6.*Sle1b* mice by staining with GC B cell markers B220, PNA and Fas/CD95. The

percentage of $B220^{+}PNA^{hi}Fas^{hi}$ GC B cells in B6.*Sle1b* males and females was significantly higher compared to their B6 control counterparts (Fig. 2A). Female mice of each genotype also had elevated percentages of $B220^{+}PNA^{hi}Fas^{hi}$ GC B cells compared to their male counterparts (Fig. 2A). We also performed immunohistological analysis in which spleen sections obtained from 6–9 month old B6 and B6.*Sle1b* female mice were stained with anti-IgD (blue) and PNA (brown). Consistent with the flow cytometry data, we found increased frequencies of $IgD^{neg}PNA^{+}$ GCs consisting of predominantly large GCs in B6.*Sle1b* female mice (lower two panels, Fig. 2C) compared to less frequent and significantly smaller GCs in B6 controls (upper two panels, Fig 2C).

Next, to evaluate whether the increased Spt-GCs in B6.*Sle1b* mice resulted from a generalized defect in immune responsiveness of B cells expressing *Sle1b*, we immunized 5–6 wk old B6 and B6.*Sle1b* mice with the TD-Ag sheep red blood cells (SRBC). The anti-SRBC stimulated GC response was determined 12 days after immunization. We did not find any significant difference in the percentage of $B220^{+}PNA^{hi}Fas^{hi}$ GC B cells (rectangular gates, Fig. 2B) upon SRBC challenge either between B6.*Sle1b* and B6 controls, or between males (blue) and females (red) within each genotype (right panel, Fig. 2B). Whereas we observed elevated frequency and size of Spt-GCs in 6–9 month old B6.*Sle1b* female mice compared to age-matched B6 female controls (Fig. 2C), similar immunohistological analysis of SRBC-immunized B6 and B6.*Sle1b* spleens revealed no difference in the frequency and size of $IgD^{neg}PNA^{+}$ GCs between B6.*Sle1b* and B6 females (Fig. 2D). These data indicate that increased number of Spt-GCs in B6.*Sle1b* mice was not the result of a generalized defect in the response of B cells expressing *Sle1b*.

Significantly higher spontaneously activated T_{FH} (Spt-T_{FH}) cells in B6.Sle1b mice

Given the increased percentage of spontaneously activated CD4 T cells in B6.*Sle1b* mice (Fig. 1C and D) we next sought to evaluate whether B6.*Sle1b* mice had an elevated percentage of spontaneously activated T_{FH} (named Spt-T_{FH}) cells. Flow cytometric analysis of splenocytes from 6–9 month old B6 and B6.*Sle1b* mice using Abs against the T_{FH} cell specific markers CD4, CXCR5 and PD-1 exhibited significantly higher percentage of $CD4^{+}CXCR5^{hi}PD\text{-}1^{hi}$ Spt-T_{FH} cells in B6.*Sle1b* mice (males and females) compared to B6 male and B6 female controls (Fig. 3A). In both B6 and B6.*Sle1b* mice, females also had significantly higher percentage of Spt-T_{FH} cells compared to males (Fig. 3A).

We also examined the T_{FH} cell response in SRBC-immunized 5–6 wk old B6 and B6.*Sle1b* mice 12 days after immunization. We found no significant difference in the percentage of $CD4^{+}CXCR5^{hi}PD\text{-}1^{hi}$ T_{FH} cells between B6.*Sle1b* mice and B6 controls (Fig. 3B). No significant difference was observed between males (blue) and females (red) of each genotype at this age (Fig. 3B). These data are consistent with the anti-SRBC GC B cell response (Fig. 2B).

To study the anatomical location of $CD4^{+}CXCR5^{hi}PD\text{-}1^{hi}$ Spt-T_{FH} cells shown in Fig. 3A, we stained spleen sections from 6–9 month old B6 and B6.*Sle1b* females with Abs against IgD (blue), CD4 (red) and PD-1 (green). We defined GC by the absence of IgD staining in IgD^{+} B cell follicles as IgD is down regulated in GC B cells (dashed lines, 1st column, Fig. 3C). Consistent with flow cytometry data we found significantly higher number of $CD4^{+}$ (lower panel, 2nd column) and $PD\text{-}1^{hi}$ (lower panel, 3rd column) T_{FH} cells in B6.*Sle1b* GCs as evidenced by the overlapped yellow staining (overlay, 4th column) compared to B6 controls (top row, Fig. 3C).

We also evaluated whether increased numbers of Spt-GCs and Spt-T_{FH} cells in B6.*Sle1b* mice could result from the decrease in $CD4^{+}Foxp\text{-}3^{+}$ T regulatory (Treg) cells. By performing flow cytometric and immunohistological analyses we found no difference

between the two strains in the frequency of $CD4^+Foxp\text{-}3^+$ Tregs within and outside of GCs (Supplementary Fig. 1).

B and T cell abnormalities occur at early age in B6.Sle1b mice

Next, we examined whether the spontaneous responses that we observed in 6–9 month old B6.Sle1b mice also occurred at earlier time points. Splenocytes from 2–3 month old unimmunized female B6.Sle1b mice and B6 controls were analyzed for spontaneous GC, T_{FH} cell and ANA-specific AFC responses. While the overall responses in these mice were lower at these earlier time points compared to later time (i.e., 6–9 month old) we found the difference in the percentages of $B220^+Fas^+PNA^{hi}$ GC B cells in B6.*Sle1b* mice compared to sex- and age-matched B6 controls statistically significant at the age of 3 months (Fig. 4A). The percentage of $CD4^+CXCR5^{hi}PD\text{-}1^{hi}$ T_{FH} cells in B6.*Sle1b* mice was also increased compared to B6 controls beginning at 2 months of age (Fig. 4B). The difference in the number of autoantibody producing AFCs was not statistically significant at this stage but 25 to 50% B6.Sle1b mice had elevated numbers of ds-DNA, histone and nucleosome-specific AFCs compared to B6 controls at 3 months old (data not shown). These data indicate that the alteration of peripheral tolerance at the GC checkpoint in the presence of *Sle1b* initiates at the earlier time point (2–3 months), which peaks at 6–9 months old.

Increased Bcl-6 expressing B cells and CD4 helper T cells in B6.Sle1b mice

Bcl-6 is considered to be a master transcriptional regulator for GC B cells (48–51) and T_{FH} cells (52–54). Given the elevated numbers of Spt-GCs and Spt-T_{FH} cells in the presence of *Sle1b*, we evaluated whether B6.*Sle1b* mice harbored an increased percentage of Bcl-6 expressing B cells and CD4 helper T cells. Flow cytometric analysis of splenocytes obtained from 6–9 month old B6 and B6.*Sle1b* mice was performed through surface staining with B220 and anti-CD4, and intracellular staining with anti-Bcl-6. The percentage of $B220^+Bcl\text{-}6^+$ B cells (Fig. 5A) and $CD4^+Bcl\text{-}6^+$ T cells (Fig. 5C) in B6.*Sle1b* females were significantly higher compared to B6.*Sle1b* males and B6 males and B6 females. No difference was observed between B6 males and B6 females, and B6 males versus B6.*Sle1b* males.

Furthermore, to determine the follicular-GC (i.e., Spt-GC) vs extrafollicular localization of $B220^+Bcl\text{-}6^+$ B cells and $CD4^+Bcl\text{-}6^+$ T cells in the spleen, immunohistological analysis was performed on two consecutive spleen sections obtained from 6–9 month old B6 and B6.*Sle1b* females. One was stained with the GC B cell marker GL7 and anti-Bcl-6 (Fig. 5B). The other was stained with anti-CD4 and anti-Bcl-6 (Fig. 5D). We found elevated Bcl-6 expressing B cells (Fig. 5B) and T cells (Fig. 5D) in B6.*Sle1b* mice, predominantly located within GCs as evidenced by the overlapped yellow staining in the overlay images (3^{rd} column, Fig. 5B and D) with a very few such cells in the extrafollicular (EF) location (i.e., T cell zone, marginal zone and red pulp) outside of GCs.

Follicular-germinal center (F-GC) versus extrafollicular (EF) spontaneous B cell proliferation in the presence or absence of Sle1b

Next, we evaluated spontaneous B cell proliferation in the follicular-germinal center (F-GC, also designated as Spt-GC) versus extrafollicular (EF) regions in the spleens of B6 and B6.*Sle1b* mice. EF areas included T cell zone, marginal zone and red pulp in the spleen. Six to nine month old B6 and B6.*Sle1b* female mice were injected with BrdU (0.6 mg/mouse) 12 hrs and 1–2 hrs prior to sacrifice to obtain spleens for analysis. Spleen sections obtained from B6 and B6.*Sle1b* mice were stained with anti-IgD (blue) and anti-BrdU (brown). GCs were characterized by the absence of IgD staining within IgD^+ follicles. Low (100×) and high (200×) magnification representative images shown in Fig. 6A revealed significantly higher number of $BrdU^+$ cells in B6.*Sle1b* mice compared to B6 controls. Interestingly,

BrdU$^+$ cells were predominantly located in F-GCs with a very small number of BrdU$^+$ cells in EF regions outside of F-GCs (Fig. 6A).

We performed a semi quantitative analysis in which we counted BrdU$^+$ cells in F-GC and EF regions at ×100 original magnification from 5 B6 and 5 B6.*Sle1b* female mice. This analysis revealed significantly higher number of BrdU$^+$ cells in F-GCs compared to EF regions in both B6 and B6.*Sle1b* mice (Fig. 6B). Whereas we did not observe significant difference in BrdU$^+$ cells in EF regions between B6 and B6.*Sle1b* mice we found B6.*Sle1b* mice had significantly higher BrdU$^+$ cells in F-GCs/Spt-GCs relative to B6 controls (Fig. 6B). Similar analysis of SRBC-immunized 5–6 week old B6 and B6.*Sle1b* female mice performed 12 days after immunization showed no difference in the number of BrdU$^+$ cells in F-GCs and EF regions (Fig. 6C and not shown) indicating no generalized defect of B6.*Sle1b* B cell proliferation against TD-Ag.

Proliferating cells within the GCs are believed to be primarily B cells. However, it is not clear whether the increased number of Spt-T_{FH} cells in Spt-GCs of B6.*Sle1b* mice (Fig. 3) could result from the proliferation of CD4 T cells located within GCs. To address this issue, we performed immunohistological analysis on two consecutive spleen sections obtained from 6–9 month old B6 and B6.*Sle1b* females. One was stained with GL7 (green, 1st column) and anti-BrdU (red, 2nd column, Fig. 6D) and the other was stained with anti-CD4 (green, 1st column) and anti-BrdU (red, 2nd column, Fig. 6E). While GL7$^+$ B cells colocalized with BrdU staining as judged by the yellow overlapped staining (3rd column, Fig. 6D) we did not observe such overlapped yellow staining with CD4 and BrdU (3rd column, Fig. 6E). Additionally, when we stained spleen sections from B6.*Sle1b* and B6 control mice with anti-IgD (blue), GL7 (green) and Ki67 (red), a cell proliferation marker, we found analogous results as in Fig. 6D showing increased numbers of Ki67$^+$ cells in B6.*Sle1b* relative to B6 control mice (Fig. 6F). Together, these data indicate that BrdU$^+$ and Ki67$^+$ proliferating cells in GCs are B cells and not CD4 T cells. Also, these data together with results shown in Fig. 3C indicate that the increased number of CD4 T cells in 6–9 month old B6.*Sle1b* GCs is due to spontaneously activated and fully differentiated T_{FH} cells.

Elevated numbers of Spt-GCs and Spt-T_{FH} cells in B6.Sle1b mice strongly correlate with increased number of ANA-specific AFCs

To evaluate whether increased numbers of Spt-GCs and Spt-T_{FH} cells in B6.*Sle1b* mice correlated with an increased ANA-specific AFC response, we first measured the number of total IgM and IgG-producing AFCs in spleen samples from 6–9 month old B6 and B6.*Sle1b* mice through ELISpot assay. The number of IgM- and IgG-producing AFCs in B6.*Sle1b* females was significantly higher compared to B6.*Sle1b* males and B6 males and B6 females (Fig. 7A). Significant difference was also observed between males and females of each genotype in IgG-producing AFCs. Consistent with the anti-SRBC GC B cell response (Fig. 2B and D) we did not observe any significant difference between B6 and B6.*Sle1b* mice in SRBC-specific IgM and IgG AFCs (Fig. 7B) 12 days after SRBC immunization. By staining with MOMA-1 (blue), which stains for metalophillic macrophages and defines the border between follicle and marginal zone, anti-CD138 (red), a marker for AFCs and anti-IgG (green) we showed elevated number of CD138$^+$IgG$^+$AFCs located both in the red pulp areas and in the bridging channels of female B6.*Sle1b* spleens compared to lower number of these cells in B6 controls located primarily in the bridging channels (Fig. 7C).

To determine whether increased Spt-GCs and total IgM and IgG AFCs in B6.*Sle1b* mice led to elevated numbers of ANA-specific AFCs, we measured ds-DNA-, histone- and nucleosome-specific AFCs by ELISpot assay. We found the numbers of AFCs with each of these specificities (Fig. 7D–F) were significantly higher in B6.*Sle1b* females compared to

B6.*Sle1b* males, B6 males, and B6 females. No difference was observed between B6.*Sle1b* males and B6 males or B6 males versus B6 females in ds-DNA and nucleosome-specific AFCs. We, however, observed significant difference between B6.*Sle1b* males and B6 males in histone-specific AFCs (Fig. 7E). Interestingly, we further observed that the increased numbers of ds-DNA-, histone- and nucleosome-specific AFCs strongly correlated with elevated numbers of GC B cells in B6.*Sle1b* mice (Fig. 7G–I).

Elevated Spt-GCs and ANA-specific AFCs in B6.Sle1b female mice led to increased serum ANA titers

To examine whether the elevated Spt-GC and AFC responses in B6.*Sle1b* mice correlated with increased serum ANA titers, we first measured ds-DNA-, histone- and nucleosome-specific total (IgM + IgG) Ab titers in sera collected from 6–9 month old B6 and B6.*Sle1b* mice (Fig. 8A–C). These titers were found to be significantly higher in B6.*Sle1b* mice compared to B6 controls. Histone-specific Abs were also significantly increased in B6.*Sle1b* females compared to B6.*Sle1b* males. No difference was observed between B6 males and B6 females. These data were consistent with results obtained in the ANA detection assay using ANA Hep-2 substrate slides. In this assay, we found significantly higher intensity of nuclear staining with sera from B6.*Sle1b* females compared to background staining in B6 females (data not shown).

Next, we evaluated IgG subclass specific ANA titers in 6–9 month old B6 and *Sle1b* mice. IgG1 ANA titers remained similar between the four groups of mice (data not shown). In contrast, B6.*Sle1b* female mice had significantly higher titers of IgG2c Abs specific for ds-DNA, histone and nucleosome compared to B6.*Sle1b* males, B6 males and B6 females (Fig. 8D–F). We also observed significantly increased IgG2b Abs specific for nucleosome in B6.*Sle1b* females (Fig. 8G). Finally, the increased IgG2c/2b ANA titers were strongly correlated with the increased number of Spt-GCs in B6.*Sle1b* mice (Fig. 8H–K).

Reduced GC response characteristic of Ars-DNA dual-reactive HKIR B cells was reversed in the presence of Sle1b

Data described above suggest that peripheral tolerance checkpoints that regulate Spt-GC formation and activation of CD4 helper T cells, including T_{FH} cells, are disrupted in the presence of *Sle1b*, which may contribute to the development of autoantibody producing AFCs and memory B cells. To determine the role and nature of self-Ags in Spt-GC formation and the alteration of the GC tolerance checkpoint by the *Sle1b* sub-locus, we used an adoptive transfer system in which we transferred Ars and DNA-dual-reactive HKIR B cells into syngenic recipients (40–42). We previously showed that dual-reactive HKIR B cells can enter GCs upon immunization with Ars-conjugated foreign antigen (i.e., Ars-KLH) but due to their autoreactivity (DNA-reactivity) these cells are negatively regulated and prevented from expanding in GCs presumably by a GC tolerance checkpoint (40–42). Therefore, the HKIR model is ideal to study the effects of *Sle1b* on GC B cell tolerance pathways of nuclear-Ag-specific B cells.

We transferred purified B cells (2×10^6) from B6.HKIR and B6.HKIR × B6.*Sle1b* (named HKIR.*Sle1b*) female mice into syngenic B6 × B6.*Sle1b* (B6.*Sle1b*$^{+/-}$) female recipients that had been immunized with Ars-KLH one wk prior to transfer. B6.*Sle1b*$^{+/-}$ mice were used as recipients to avoid allo-rejection and B6.*Sle1b*$^{+/-}$ mice do not display any autoimmune features, as the influence of *Sle1b* on lymphoid and accessory cell function is recessive (1). We used the anti-clonotypic mAb E4 to detect dual-reactive HKIR B cells as described (40–42). E4-specific primary AFC and GC responses were determined in spleen samples obtained on day 5 after cell transfer. Flow cytometric analysis of splenocytes revealed a significant increase in the percentage of donor-derived $E4^+PNA^+$ GC B cells in

HKIR.*Sle1b*→ B6.*Sle1b*$^{+/-}$ mice compared with HKIR→ B6.*Sle1b*$^{+/-}$ controls (Fig. 9A–B). These data were consistent with immunohistology results showing more E4^{+} (red) and E4^{+}PNA^{+} (yellow) cells in GCs of HKIR.*Sle1b*→ B6.*Sle1b*$^{+/-}$ mice (lower panel, Fig. 9C) compared with HKIR→ B6.*Sle1b*$^{+/-}$ controls (upper panel, Fig. 9C). The E4-specific short-lived AFC response to Ars was also evaluated by ELISpot assay in the recipient mice. We did not, however, observe any significant difference between HKIR.*Sle1b*→ B6.*Sle1b*$^{+/-}$ and HKIR→ B6.*Sle1b*$^{+/-}$ mice in producing E4-specific short-lived AFCs (data not shown).

Sle1b expression in B cells, but not in T cells, resulted in elevated Spt-GCs, T_{FH} cells, ANA-specific AFCs and ANAs in B6.Sle1b mice

Next, we evaluated whether phenotypic changes that were observed in T cells (i.e., activation of T cells and increased percentage of GC T_{FH} cells) in B6.*Sle1b* mice resulted from the primary effect of *Sle1b* on T cells or were they influenced by B cells expressing *Sle1b*. Using μMT and TCRβδ$^{-/-}$ mice which lack B and T cells respectively, we generated mixed bone marrow (BM) chimeric mice where in one group of mice (i.e., B6.*Sle1b* + B6.μMT marrow → B6.μMT) all reconstituted B cells expressed *Sle1b* while in the other group (i.e., B6.*Sle1b* + B6.TCRβδ$^{-/-}$ marrow → B6.TCRβδ$^{-/-}$) all reconstituted T cells expressed *Sle1b* in the presence of chimeric accessory compartments. We used B6 + B6.μMT BM marrow → B6.μMT and B6 + B6.TCRβδ$^{-/-}$ marrow → B6.TCRβδ$^{-/-}$ chimeras as controls. Only female mice were used for these experiments. These mice were rested for six months before analyzing for the development of Spt-GCs, T_{FH} cells, autoantibody producing AFCs and ANAs.

Flow cytometry analysis on spleen cells obtained from these mice revealed significantly higher percentages of B220^{+}Fas^{+}PNA^{hi} GC B cells (Fig. 10A) and CD4^{+}CXCR5^{hi}PD-1^{hi} T_{FH} cells (Fig. 9B) in B6.*Sle1b* + B6.μMT BM → B6.μMT mice compared to B6 + B6.μMT BM → B6.μMT controls. Interestingly, increased frequency of GC B cells and T_{FH} cells was not observed in B6.*Sle1b* + B6.TCRβδ$^{-/-}$ → B6.TCRβδ −/− chimeras where all T cells expressed *Sle1b* and no significant difference was observed between B6 + B6.TCRβδ$^{-/-}$ → B6.TCRβδ$^{-/-}$ and B6.*Sle1b* + B6.TCRβδ$^{-/-}$ → B6.TCRβδ$^{-/-}$ mice (Fig. 10A–B). These results were consistent with immunohistological data obtained from spleen sections showing increased frequencies of IgD^{neg}PNA^{+} GCs with predominantly large GCs in B6.*Sle1b* + B6.μMT → B6.μMT mice (upper right, Fig. 10C) compared to other three groups of mice showing less frequent and significantly smaller GCs (Fig. 10C). The number of CD4^{+} T cells also appeared to be increased in B6.*Sle1b* + B6.μMT BM → B6.μMT mice compared to other three groups (Fig. 10D).

By performing ELISPot assay, we further observed that B6.*Sle1b* + B6.μMT → B6.μMT mice had significantly higher ds-DNA-, histone- and nucleosome-specific AFCs compared to B6 + B6.μMT → B6.μMT control mice (Fig. 10E–G). In agreement with the GC B cell and T_{FH} cell data (Fig. 10A–B) we did not find any difference in ANA-specific AFCs between B6 + B6.TCRβδ −/− → B6.TCRβδ −/− and B6.*Sle1b* + B6.TCRβδ −/− → B6.TCRβδ −/− mice (Fig. 10E–G). Analogous to the AFC data we found significantly higher ds-DNA-, histone- and nucleosome-specific Abs in B6.*Sle1b* + B6.μMT → B6.μMT mice compared to other three groups of mice (Fig. 10H–J).

These data, together with results described above (Fig. 9) indicate that the alteration of the GC checkpoint by *Sle1b* is B cell autonomous and the effect of *Sle1b* on T cells appears to be secondary to the B cell defect.

Discussion

In this study, we determined the influence of the *Sle1b* genomic interval, which contains the lupus associated NZM2410/NZW SLAM family genes, on the GC tolerance pathway or checkpoint which may lead to the development of elevated ANA titers. We utilized spontaneously developed, B cell adoptive transfer and bone marrow transfer models in order to provide a comprehensive analysis of the effects of *Sle1b* on the GC checkpoint. In the spontaneously developed GC model, we found significantly increased percentage of GC B cells and GC T_{FH} cells in B6.*Sle1b* female mice relative to B6 female controls. Strong correlation was observed between the elevated numbers of Spt-GCs in B6.*Sle1b* mice and the increased numbers of ds-DNA-, histone-, and nucleosome-specific AFCs, as well as high titers of serum ANAs. Using the adoptive transfer model, we found an augmented GC response of Ars-DNA dual-reactive HKIR B cells in the presence of *Sle1b*. Additionally, by generating mixed bone marrow chimeras, we observed that the effect of *Sle1b* on the alteration of the GC tolerance checkpoint was B cell autonomous and the effect of *Sle1b* on T cells including GC T_{FH} cells appeared to be secondary to the B cell defect. Together, these data suggest that genes located in *Sle1b* contribute to the alteration of the GC checkpoint by primarily affecting B cells leading to enhanced Spt-GCs, Spt-T_{FH} cells and the generation of autoantibody-producing AFCs.

Given the roles of SLAM family co-stimulatory molecules in regulating cellular and humoral immunity (14, 15, 55, 56) and the association of SLAM family genes located in *Sle1b* with lupus (7–9), these genes are strong candidates for perturbing peripheral tolerance checkpoints (i.e., the GC checkpoint) in B6.*Sle1b* mice. While the data presented here suggest that the lupus-associated SLAM family genes in *Sle1b* are presumably responsible for the alteration of peripheral tolerance at the GC checkpoint, previous studies using the HEL immunoglobulin transgenic mouse system revealed that the *Ly108.1* isoform of the *Ly108* gene in *Sle1b* alters early or central B cell tolerance (8). Recent studies by Keszei et al. implicated the *Ly108.1* gene in altering peripheral tolerance (9). The current studies together with the available literature suggest that the *Ly108.1* isoform expressed by B6.*Sle1b* mice may alter both central and peripheral tolerance checkpoints. The polymorphisms in different members of SLAM family genes may also coordinate in altering B cell tolerance at different checkpoints.

One of the intriguing questions in studies of autoreactive B cell activation in autoimmune mouse models is where the site of a break in tolerance occurs. Whereas defects in the central tolerance checkpoint are proposed in causing autoimmunity, the development of autoantibody producing long-lived IgG^+ AFCs and memory B cells in lupus cannot be explained by a defect in the central tolerance checkpoint alone as these cells are usually generated in GCs formed in peripheral lymphoid organs. Therefore, peripheral tolerance checkpoints (i.e., the GC checkpoint) may play a crucial role in the prevention of autoreactive B cells from developing into long-lived AFCs and memory B cells, which can persist for years. Numerous autoimmune mouse models, including (NZB/NZW) F1, BXSB, and *sanroque*, spontaneously develop GCs in the absence of an infection or immunization (24, 33, 36) and all of these mouse models develop autoantibodies against nuclear-self-antigens. However, the role of a dysregulated GC tolerance pathway in autoantibody production in these mice is unclear. Our current results in B6.*Sle1b* mice demonstrate that increased GC formation is directly correlated to increased numbers of ds-DNA-, histone-, and nucleosome-specific AFCs, as well as increased ANA titers. Direct evidence for the break in peripheral tolerance at the GC checkpoint is further demonstrated by the increase in HKIR B cells populating GCs in the presence of *Sle1b*. These results implicate a dysregulated GC checkpoint or pathway in ANA production and autoimmunity in B6.*Sle1b* mice.

Activated B cells can also develop into memory B cells and plasma cells independent of the GC outside of the follicle (58–60). The AFCs generated from this extrafollicular pathway tend to be short-lived and the memory B cells remain largely un-switched (57). Several studies have implicated the role of the extrafollicular pathway of B cell activation in autoimmunity. Autoreactive B cells in MRL.Fas^{lpr} mice do not involve the GC pathway, but instead they undergo somatic hypermutation in the T cell zone (58, 59). The (NZB/NZW) F1 mice develop short-lived plasmablasts via an extrafollicular pathway that are autoreactive for ds-DNA and contribute to the autoimmunity (60). Our data indicate that the *Sle1b* sub-locus primarily affects the GC checkpoint leading to increased numbers of ANA-specific and class-switched IgG$^+$ AFCs and ANAs. While a role of extrafollicular ANA-specific B cells cannot be entirely discounted in our autoimmune model, our data suggest that a major contributor to the break in peripheral tolerance leading to the production of ANA in B6.*Sle1b* mice is through the alteration of the GC tolerance pathway.

T_{FH} cells play an integral role in the formation of the GC as well as for the maturation and development of GC B cells into long-lived AFCs and memory B cells. Several studies have implicated dysregulated T_{FH} cells in the development of autoimmunity (12, 33, 35–37). The autoimmune mouse models, including mice expressing two copies of TLR7 (i.e., BXSB.*yaa* mice) and *sanroque* mice have increased numbers of T_{FH} cells coincident with high titers of ANAs (33, 36, 37). B6.*Sle1b* mice have increased numbers of Spt-GC B cells along with a significantly higher numbers of Spt-T_{FH} cells. Consistent with studies in other autoimmune mice (33, 36, 37), our current data implicate a role for dysregulated T_{FH} cell numbers in developing autoantibody producing IgG$^+$ AFCs and high titers of ANAs in B6.*Sleb* mice.

Sle1 or *Sle1b* appears to affect both B and T cells (5, 7–9). In support for a predominant B cell intrinsic effect, Kumar et al. have demonstrated that the presence of the *Ly108.1* isoform from the *Sle1* locus renders B cells unresponsive to normal regulation at early B cell tolerance checkpoints (8). We previously showed that the presence of *Sle1* on HKIR B cells enables them to escape GC tolerance mechanisms and allows increased participation of HKIR B cells expressing *Sle1* in the GC response (42). Our current results from B cell adoptive transfer experiments (Fig. 9) showing increased participation of HKIR.*Sle1b* B cells in the anti-Ars GC response provide evidence for a B cell intrinsic effect on the breach in peripheral tolerance at the GC checkpoint. These results are in agreement with our bone marrow chimeric data (Fig. 10) showing B cell autonomous effect of *Sle1b* on increased Spt-GCs, T_{FH} cells, and ANA-specific AFCs and Abs. In contrast, studies by Keszei et al. recently suggested the role for peripheral CD4$^+$ T cells from B6.*Sle1b* mice in autoantibody responses by transferring purified *Sle1b* CD4$^+$ T cells or CD62L$^+$ naive CD4$^+$ T cells into *bm12* mice (9). However, our bone marrow chimeric data revealed no primary effect of *Sle1b* on T cells (Fig. 10B) rather T cells were indirectly influenced by the expression of *Sle1b* in B cells, providing evidence for the requirement of B cell intrinsic defect caused by *Sle1b* in the development of Spt-GCs, T_{FH} cell expansion and autoantibody response.

One central theme that we observed in these studies is that only the female B6.*Sle1b* mice had the highest percentages of spontaneously formed GCs, T_{FH} numbers, ANA-specific AFCs and serum ANA titers. Even though male B6.*Sle1b* mice had higher numbers of Spt-GCs and Spt-T_{FH} cells compared to B6 males the numbers of ANA-specific AFCs were not significantly different from B6 controls. Therefore, *Sle1b* appears to have the highest penetrance in female mice. In our knowledge, this is the first thorough study showing the differences in B cell/T cell activation, GC formation, and ANA-specific AFC numbers between male and female B6.*Sle1b* mice. Our results are in accordance with previous report by Grimaldi et al. showing that estrogen alters thresholds for B cell apoptosis and activation (61). The importance of sex hormones in the immune system homeostasis is evident through differences between males and females in B6 mice, as female B6 mice tend to have higher

spontaneously activated phenotypes. This is consistent with the findings that an overwhelming percentage of people with autoimmune diseases are female. We cannot rule out the potential role of female chromosome as the inactivation of the second X-chromosome in females can sometimes be incomplete leading to dysregulated gene repression (62) that may contribute to enhanced Spt-GC, Spt-T_{FH} and ANA titers observed in female mice in our studies. We are also unable to exclude the potential protective role of male hormones or chromosome in this process. It is of great interest to further dissect the role of the lupus-associated SLAM family genes in conjunction with sex hormones (i.e., estrogen) or chromosomes in breaking peripheral B cell tolerance at the GC checkpoint leading to the development of autoantibody producing long-lived AFC and memory B cells.

Supplementary Material

Refer to Web version on PubMed Central for supplementary material.

Acknowledgments

We thank Drs. Cathie Calkins and Chris Snyder for their critical reading of the manuscript and constructive comments. We also thank Dr. Chetna Soni from our laboratory for her indirect contribution. We thank Dr. Tim Manser (Thomas Jefferson University, Philadelphia, PA) for providing the HKIR mice and Dr. Edward Wakeland for providing B6.*Sle1b* mice.

These studies were supported by grants from the NIH (AI091670) and from the Arthritis National Research Foundation to Z.S.M.R.

Non standard abbreviations

GC	germinal center
Spt-GC	spontaneous germinal center
AFC	antibody forming cell
MZ	marginal zone
PNA	peanut lectin (agglutinin)
ANA	anti-nuclear antibody
SRBC	sheep red blood cells
T_{FH}	follicular helper T cells
Spt-T_{FH}	spontaneously activated follicular helper T cells

References

1. Morel L, Rudofsky UH, Longmate JA, Schiffenbauer J, Wakeland EK. Polygenic control of susceptibility to murine systemic lupus erythematosus. Immunity. 1994; 1:219–229. [PubMed: 7889410]
2. Morel L, Croker BP, Blenman KR, Mohan C, Huang G, Gilkeson G, Wakeland EK. Genetic reconstitution of systemic lupus erythematosus immunopathology with polycongenic murine strains. Proc. Natl. Acad. Sci. U. S. A. 2000; 97:6670–6675. [PubMed: 10841565]
3. Morel L, Wakeland EK. Lessons from the NZM2410 model and related strains. Int. Rev. Immunol. 2000; 19:423–446. [PubMed: 11016426]
4. Mohan C, Alas E, Morel L, Yang P, Wakeland EK. Genetic dissection of SLE pathogenesis. Sle1 on murine chromosome 1 leads to a selective loss of tolerance to H2A/H2B/DNA subnucleosomes. J. Clin. Invest. 1998; 101:1362–1372. [PubMed: 9502778]

5. Sobel ES, Satoh M, Chen Y, Wakeland EK, Morel L. The major murine systemic lupus erythematosus susceptibility locus Sle1 results in abnormal functions of both B and T cells. J. Immunol. 2002; 169:2694–2700. [PubMed: 12193743]
6. Morel L, Blenman KR, Croker BP, Wakeland EK. The major murine systemic lupus erythematosus susceptibility locus, Sle1, is a cluster of functionally related genes. Proc. Natl. Acad. Sci. U. S. A. 2001; 98:1787–1792. [PubMed: 11172029]
7. Wandstrat AE, Nguyen C, Limaye N, Chan AY, Subramanian S, Tian XH, Yim YS, Pertsemlidis A, Garner HR Jr, Morel L, Wakeland EK. Association of extensive polymorphisms in the SLAM/CD2 gene cluster with murine lupus. Immunity. 2004; 21:769–780. [PubMed: 15589166]
8. Kumar KR, Li L, Yan M, Bhaskarabhatla M, Mobley AB, Nguyen C, Mooney JM, Schatzle JD, Wakeland EK, Mohan C. Regulation of B cell tolerance by the lupus susceptibility gene Ly108. Science. 2006; 312:1665–1669. [PubMed: 16778059]
9. Keszei M, Detre C, Rietdijk ST, Munoz P, Romero X, Berger SB, Calpe S, Liao G, Castro W, Julien A, Wu YY, Shin DM, Sancho J, Zubiaur M, Morse HC 3rd, Morel L, Engel P, Wang N, Terhorst C. A novel isoform of the Ly108 gene ameliorates murine lupus. J. Exp. Med. 2011; 208:811–822. [PubMed: 21422172]
10. Jennings P, Chan A, Schwartzberg P, Wakeland EK, Yuan D. Antigen-specific responses and ANA production in B6.Sle1b mice: a role for SAP. J. Autoimmun. 2008; 31:345–353. [PubMed: 18845419]
11. Croker BP, Gilkeson G, Morel L. Genetic interactions between susceptibility loci reveal epistatic pathogenic networks in murine lupus. Genes Immun. 2003; 4:575–585. [PubMed: 14647198]
12. Subramanian S, Tus K, Li QZ, Wang A, Tian XH, Zhou J, Liang C, Bartov G, McDaniel LD, Zhou XJ, Schultz RA, Wakeland EK. A Tlr7 translocation accelerates systemic autoimmunity in murine lupus. Proc. Natl. Acad. Sci. U. S. A. 2006; 103:9970–9975. [PubMed: 16777955]
13. Xie C, Patel R, Wu T, Zhu J, Henry T, Bhaskarabhatla M, Samudrala R, Tus K, Gong Y, Zhou H, Wakeland EK, Zhou XJ, Mohan C. PI3K/AKT/mTOR hypersignaling in autoimmune lymphoproliferative disease engendered by the epistatic interplay of Sle1b and FASlpr. Int. Immunol. 2007; 19:509–522. [PubMed: 17369192]
14. Cannons JL, Tangye SG, Schwartzberg PL. SLAM family receptors and SAP adaptors in immunity. Annu. Rev. Immunol. 2011; 29:665–705. [PubMed: 21219180]
15. Detre C, Keszei M, Romero X, Tsokos GC, Terhorst C. SLAM family receptors and the SLAM-associated protein (SAP) modulate T cell functions. Semin. Immunopathol. 2010; 32:157–171. [PubMed: 20146065]
16. Ma CS, Nichols KE, Tangye SG. Regulation of cellular and humoral immune responses by the SLAM and SAP families of molecules. Annu. Rev. Immunol. 2007; 25:337–379. [PubMed: 17201683]
17. Koh AE, Njoroge SW, Feliu M, Cook A, Selig MK, Latchman YE, Sharpe AH, Colvin RB, Paul E. The SLAM family member CD48 (Slamf2) protects lupus-prone mice from autoimmune nephritis. J. Autoimmun. 2011; 37:48–57. [PubMed: 21561736]
18. Berek C, Milstein C. Mutation drift and repertoire shift in the maturation of the immune response. Immunol. Rev. 1987; 96:23–41. [PubMed: 3298007]
19. Weiss U, Rajewsky K. The repertoire of somatic antibody mutants accumulating in the memory compartment after primary immunization is restricted through affinity maturation and mirrors that expressed in the secondary response. J. Exp. Med. 1990; 172:1681–1689. [PubMed: 2124253]
20. Manser T, Wysocki LJ, Margolies MN, Gefter ML. Evolution of antibody variable region structure during the immune response. Immunol. Rev. 1987; 96:141–162. [PubMed: 3298006]
21. Kelsoe G. Life and death in germinal centers (redux). Immunity. 1996; 4:107–111. [PubMed: 8624801]
22. Pulendran B, van Driel R, Nossal GJ. Immunological tolerance in germinal centres. Immunol. Today. 1997; 18:27–32. [PubMed: 9018971]
23. Pulendran B, Kannourakis G, Nouri S, Smith KG, Nossal GJ. Soluble antigen can cause enhanced apoptosis of germinal-centre B cells. Nature. 1995; 375:331–334. [PubMed: 7753199]

24. Luzina IG, Atamas SP, Storrer CE, daSilva LC, Kelsoe G, Papadimitriou JC, Handwerger BS. Spontaneous formation of germinal centers in autoimmune mice. J. Leukoc. Biol. 2001; 70:578–584. [PubMed: 11590194]
25. Diamond B, Scharff MD. Somatic mutation of the T15 heavy chain gives rise to an antibody with autoantibody specificity. Proc. Natl. Acad. Sci. U. S. A. 1984; 81:5841–5844. [PubMed: 6435121]
26. Diamond B, Katz JB, Paul E, Aranow C, Lustgarten D, Scharff MD. The role of somatic mutation in the pathogenic anti-DNA response. Annu. Rev. Immunol. 1992; 10:731–757. [PubMed: 1591002]
27. Shlomchik M, Mascelli M, Shan H, Radic MZ, Pisetsky D, Marshak-Rothstein A, Weigert M. Anti-DNA antibodies from autoimmune mice arise by clonal expansion and somatic mutation. J. Exp. Med. 1990; 171:265–292. [PubMed: 2104919]
28. Shlomchik MJ, Marshak-Rothstein A, Wolfowicz CB, Rothstein TL, Weigert MG. The role of clonal selection and somatic mutation in autoimmunity. Nature. 1987; 328:805–811. [PubMed: 3498121]
29. Olee T, Lu EW, Huang DF, Soto-Gil RW, Deftos M, Kozin F, Carson DA, Chen PP. Genetic analysis of self-associating immunoglobulin G rheumatoid factors from two rheumatoid synovia implicates an antigen-driven response. J. Exp. Med. 1992; 175:831–842. [PubMed: 1740665]
30. Kim SJ, Zou YR, Goldstein J, Reizis B, Diamond B. Tolerogenic function of Blimp-1 in dendritic cells. J. Exp. Med. 2011; 208:2193–2199. [PubMed: 21948081]
31. Tiller T, Kofer J, Kreschel C, Busse CE, Riebel S, Wickert S, Oden F, Mertes MM, Ehlers M, Wardemann H. Development of self-reactive germinal center B cells and plasma cells in autoimmune Fc gammaRIIB-deficient mice. J. Exp. Med. 2010; 207:2767–2778. [PubMed: 21078890]
32. Vinuesa CG, Tangye SG, Moser B, Mackay CR. Follicular B helper T cells in antibody responses and autoimmunity. Nat. Rev. Immunol. 2005; 5:853–865. [PubMed: 16261173]
33. Linterman MA, Rigby RJ, Wong RK, Yu D, Brink R, Cannons JL, Schwartzberg PL, Cook MC, Walters GD, Vinuesa CG. Follicular helper T cells are required for systemic autoimmunity. J. Exp. Med. 2009; 206:561–576. [PubMed: 19221396]
34. Craft JE. Follicular helper T cells in immunity and systemic autoimmunity. Nat. Rev. Rheumatol. 2012; 8:337–347. [PubMed: 22549246]
35. King C, Tangye SG, Mackay CR. T follicular helper (TFH) cells in normal and dysregulated immune responses. Annu. Rev. Immunol. 2008; 26:741–766. [PubMed: 18173374]
36. Vinuesa CG, Cook MC, Angelucci C, Athanasopoulos V, Rui L, Hill KM, Yu D, Domaschenz H, Whittle B, Lambe T, Roberts IS, Copley RR, Bell JI, Cornall RJ, Goodnow CC. A RING-type ubiquitin ligase family member required to repress follicular helper T cells and autoimmunity. Nature. 2005; 435:452–458. [PubMed: 15917799]
37. Bubier JA, Sproule TJ, Foreman O, Spolski R, Shaffer DJ, Morse HC 3rd, Leonard WJ, Roopenian DC. A critical role for IL-21 receptor signaling in the pathogenesis of systemic lupus erythematosus in BXSB-Yaa mice. Proc. Natl. Acad. Sci. U. S. A. 2009; 106:1518–1523. [PubMed: 19164519]
38. Heltemes-Harris L, Liu X, Manser T. Progressive surface B cell antigen receptor down-regulation accompanies efficient development of antinuclear antigen B cells to mature, follicular phenotype. J. Immunol. 2004; 172:823–833. [PubMed: 14707052]
39. Liu X, Manser T. Antinuclear antigen B cells that down-regulate surface B cell receptor during development to mature, follicular phenotype do not display features of anergy in vitro. J. Immunol. 2005; 174:4505–4515. [PubMed: 15814671]
40. Alabyev B, Rahman ZS, Manser T. Quantitatively reduced participation of anti-nuclear antigen B cells that down-regulate B cell receptor during primary development in the germinal center/memory B cell response to foreign antigen. J. Immunol. 2007; 178:5623–5634. [PubMed: 17442945]
41. Rahman ZS, Alabyev B, Manser T. FcgammaRIIB regulates autoreactive primary antibody-forming cell, but not germinal center B cell, activity. J. Immunol. 2007; 178:897–907. [PubMed: 17202351]

42. Vuyyuru R, Mohan C, Manser T, Rahman ZS. The lupus susceptibility locus Sle1 breaches peripheral B cell tolerance at the antibody-forming cell and germinal center checkpoints. J. Immunol. 2009; 183:5716–5727. [PubMed: 19828626]
43. Notidis E, Heltemes L, Manser T. Dominant, hierarchical induction of peripheral tolerance during foreign antigen-driven B cell development. Immunity. 2002; 17:317–327. [PubMed: 12354384]
44. Vora KA, Tumas-Brundage KM, Lentz VM, Cranston A, Fishel R, Manser T. Severe attenuation of the B cell immune response in Msh2-deficient mice. J. Exp. Med. 1999; 189:471–482. [PubMed: 9927509]
45. Rahman ZS, Shao WH, Khan TN, Zhen Y, Cohen PL. Impaired apoptotic cell clearance in the germinal center by Mer-deficient tingible body macrophages leads to enhanced antibody-forming cell and germinal center responses. J. Immunol. 2010; 185:5859–5868. [PubMed: 20952679]
46. Cappione A 3rd, Anolik JH, Pugh-Bernard A, Barnard J, Dutcher P, Silverman G, Sanz I. Germinal center exclusion of autoreactive B cells is defective in human systemic lupus erythematosus. J. Clin. Invest. 2005; 115:3205–3216. [PubMed: 16211091]
47. Baumann I, Kolowos W, Voll RE, Manger B, Gaipl U, Neuhuber WL, Kirchner T, Kalden JR, Herrmann M. Impaired uptake of apoptotic cells into tingible body macrophages in germinal centers of patients with systemic lupus erythematosus. Arthritis Rheum. 2002; 46:191–201. [PubMed: 11817590]
48. Basso K, Dalla-Favera R. BCL6: master regulator of the germinal center reaction and key oncogene in B cell lymphomagenesis. Adv. Immunol. 2010; 105:193–210. [PubMed: 20510734]
49. Dent AL, Shaffer AL, Yu X, Allman D, Staudt LM. Control of inflammation, cytokine expression, and germinal center formation by BCL-6. Science. 1997; 276:589–592. [PubMed: 9110977]
50. Ye BH, Cattoretti G, Shen Q, Zhang J, Hawe N, de Waard R, Leung C, Nouri-Shirazi M, Orazi A, Chaganti RS, Rothman P, Stall AM, Pandolfi PP, Dalla-Favera R. The BCL-6 proto-oncogene controls germinal-centre formation and Th2-type inflammation. Nat. Genet. 1997; 16:161–170. [PubMed: 9171827]
51. Onizuka T, Moriyama M, Yamochi T, Kuroda T, Kazama A, Kanazawa N, Sato K, Kato T, Ota H, Mori S. BCL-6 gene product, a 92- to 98-kD nuclear phosphoprotein, is highly expressed in germinal center B cells and their neoplastic counterparts. Blood. 1995; 86:28–37. [PubMed: 7795234]
52. Nurieva RI, Chung Y, Martinez GJ, Yang XO, Tanaka S, Matskevitch TD, Wang YH, Dong C. Bcl6 mediates the development of T follicular helper cells. Science. 2009; 325:1001–1005. [PubMed: 19628815]
53. Yu D, Rao S, Tsai LM, Lee SK, He Y, Sutcliffe EL, Srivastava M, Linterman M, Zheng L, Simpson N, Ellyard JI, Parish IA, Ma CS, Li QJ, Parish CR, Mackay CR, Vinuesa CG. The transcriptional repressor Bcl-6 directs T follicular helper cell lineage commitment. Immunity. 2009; 31:457–468. [PubMed: 19631565]
54. Johnston RJ, Poholek AC, DiToro D, Yusuf I, Eto D, Barnett B, Dent AL, Craft J, Crotty S. Bcl6 and Blimp-1 are reciprocal and antagonistic regulators of T follicular helper cell differentiation. Science. 2009; 325:1006–1010. [PubMed: 19608860]
55. Veillette A, Latour S. The SLAM family of immune-cell receptors. Curr. Opin. Immunol. 2003; 15:277–285. [PubMed: 12787752]
56. Engel P, Eck MJ, Terhorst C. The SAP and SLAM families in immune responses and X-linked lymphoproliferative disease. Nat. Rev. Immunol. 2003; 3:813–821. [PubMed: 14523387]
57. Taylor JJ, Pape KA, Jenkins MK. A germinal center-independent pathway generates unswitched memory B cells early in the primary response. J. Exp. Med. 2012; 209:597–606. [PubMed: 22370719]
58. William J, Euler C, Christensen S, Shlomchik MJ. Evolution of autoantibody responses via somatic hypermutation outside of germinal centers. Science. 2002; 297:2066–2070. [PubMed: 12242446]
59. Shlomchik MJ, Euler CW, Christensen SC, William J. Activation of rheumatoid factor (RF) B cells and somatic hypermutation outside of germinal centers in autoimmune-prone MRL/lpr mice. Ann. N. Y. Acad. Sci. 2003; 987:38–50. [PubMed: 12727622]

60. Hoyer BF, Moser K, Hauser AE, Peddinghaus A, Voigt C, Eilat D, Radbruch A, Hiepe F, Manz RA. Short-lived plasmablasts and long-lived plasma cells contribute to chronic humoral autoimmunity in NZB/W mice. J. Exp. Med. 2004; 199:1577–1584. [PubMed: 15173206]

61. Grimaldi CM, Cleary J, Dagtas AS, Moussai D, Diamond B. Estrogen alters thresholds for B cell apoptosis and activation. J. Clin. Invest. 2002; 109:1625–1633. [PubMed: 12070310]

62. Brooks WH. X chromosome inactivation and autoimmunity. Clin. Rev. Allergy Immunol. 2010; 39:20–29. [PubMed: 19653135]

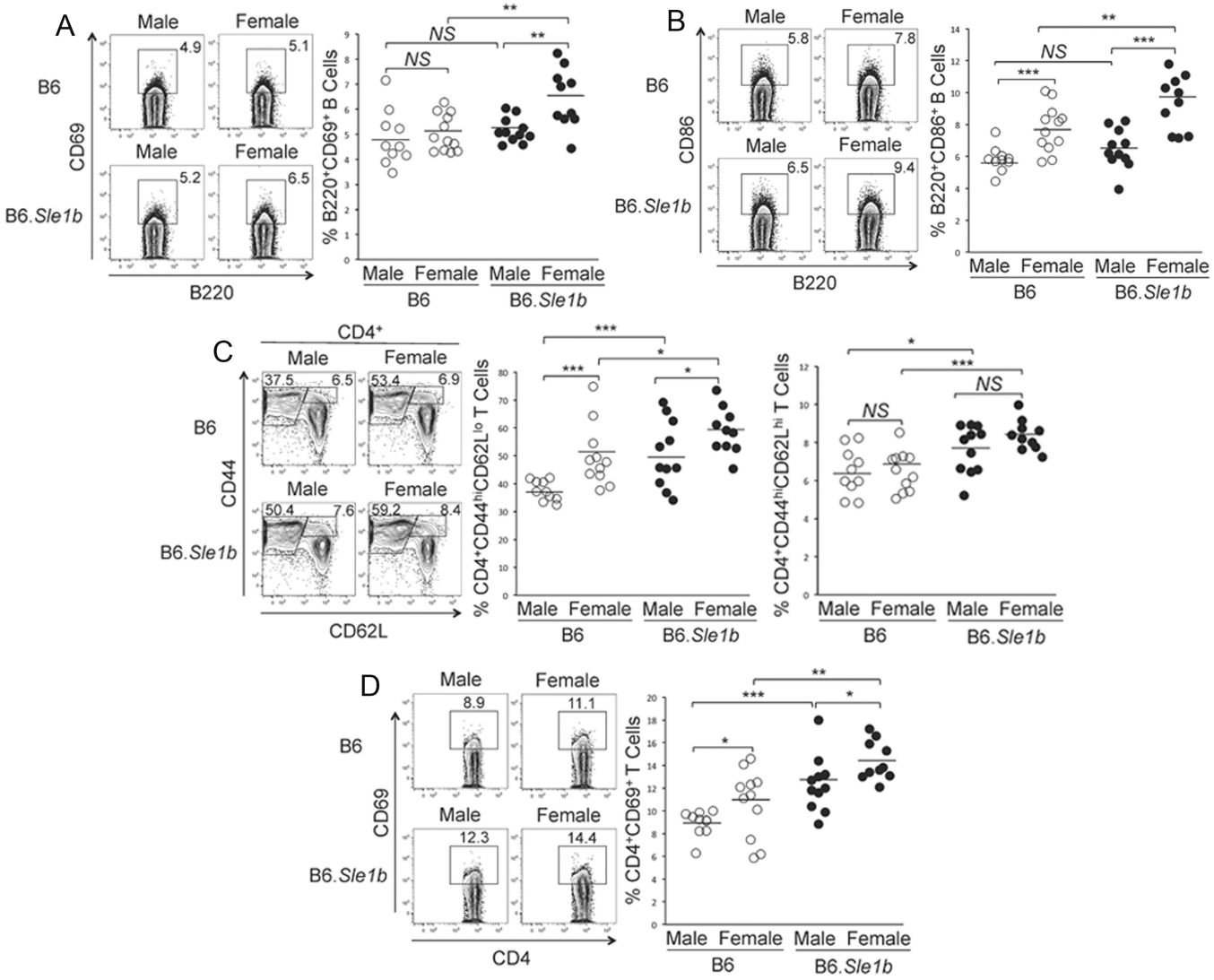

Figure 1. Increased spontaneous activation of B cells and CD4 helper T cells in B6.Sle1b female mice

Flow cytometric analysis was performed on splenocytes from 6–9 month old, sex-matched B6 and B6.*Sle1b* mice after staining for activated B cells using mAbs against B220, CD69 and CD86. The percentage of $B220^{+}CD69^{+}$ (A) and $B220^{+}CD86^{+}$ (B) activated B cells are shown in rectangular gates (left panels) and in scatter plots (right panels). Activated CD4 T cells were analyzed using antibodies against CD4, CD44, CD62L and CD69. The percentage of $CD4^{+}CD44^{hi}CD62L^{lo}$ short-lived effector and $CD4^{+}CD44^{hi}CD62L^{hi}$ effector memory helper T cells are shown in rectangular gates (left panel, C) and in scatter plots (middle and right panels, respectively, C). The percentage of $CD4^{+}CD69^{+}$ activated T cells are shown in rectangular gates (left panel, D) and in scatter plot (D, right panel). Each circle represents an individual mouse and horizontal bars represent the mean values. Statistical analysis was performed as described in Materials and Methods.

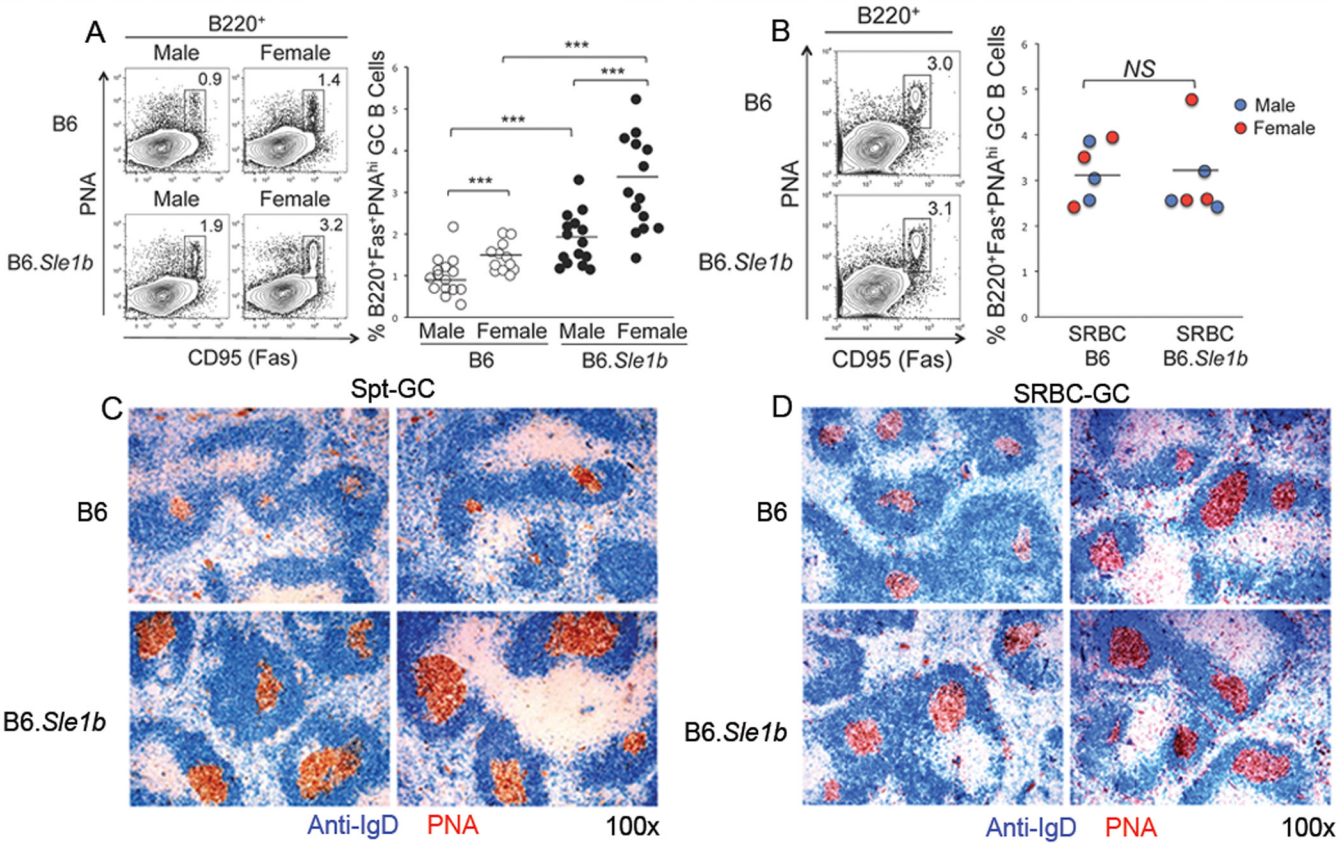

Figure 2. Elevated number of Spt-GCs in B6.Sle1b mice

(A) Flow cytometric analysis was performed on splenocytes obtained from sex matched, 6–9 month old B6 and B6.*Sle1b* mice for spontaneous GCs (Spt-GCs). The percentage of $B220^{+}ΠNA^{hi}Fas^{hi}$ GC B cells are shown in rectangular gates (left panel) and in scatter plots (right panel). (B) In a similar analysis as in (A), splenocytes obtained from 5 to 6 week old SRBC-immunized B6 and B6.*Sle1b* mice were analyzed 12 days post-immunization to show the percentage of $B220^{+}PNA^{hi}Fas^{hi}$ GC B cells in these mice. The flow cytometry plots on the left are representative images from each group while the scatter plots on the right showing the range of the GC B cell percentages. The blue dots represent male mice and the red dots represent female mice (right panel, B). Each circle represents an individual mouse and horizontal bars represent the mean values. Statistical analysis was performed as described in Materials and Methods. (C) Spleen sections obtained from 6–9 month old female B6 and B6.*Sle1b* mice were stained with anti-IgD (blue) and PNA (red). (D) Similar analysis as in (C) was performed on spleen sections obtained from SRBC-immunized 5 to 6 week old female B6 (n=6) and B6.*Sle1b* (n=6) mice 12 days post immunization. Original magnification of the images was 100×. The data shown in (C and D) represent at least 5 mice of each genotype.

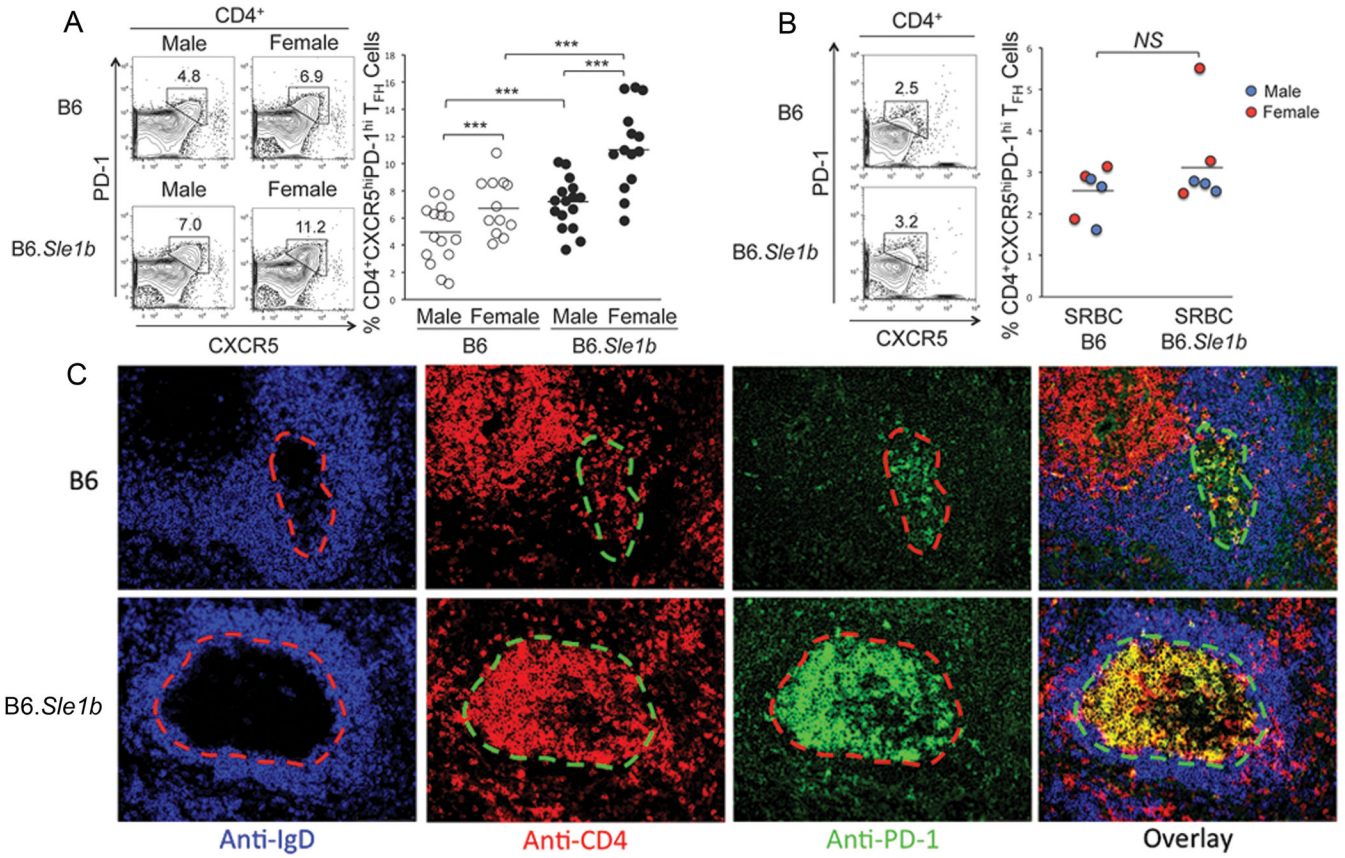

Figure 3. Elevated Spt-T_{FH} cell numbers concomitant with augmented Spt-GCs in B6.Sle1b female mice

(A) Flow cytometric analysis of splenocytes obtained from sex matched, 6–9 month old B6 and B6.*Sle1b* mice for the percentages of Spt-T_{FH} cells. (B) The percentage of T_{FH} cells from 5–6 week old SRBC-immunized B6 and B6.*Sle1b* mice were also analyzed 12 days post-immunization. (A and B) T_{FH} cells are defined as $CD4^+CXCR5^{hi}PD\text{-}1^{hi}$ and are highlighted by the rectangular gates. The flow cytometry plots on the left are representative images from each group while the scatter plots on the right showing the range of the T_{FH} cell percentages. The blue dots represent male mice and the red dots represent female mice in (B). Each circle represents an individual mouse and horizontal bars represent the mean values. Statistical analysis was performed as described in Materials and Methods. (C) Spleen sections obtained from aged 6–9 month old female B6 and B6.*Sle1b* mice were stained with anti-IgD (blue), anti-CD4 (red) and anti-PD-1 (green). Representative images from 5 mice of each genotype are shown where original magnification of the images was 200×.

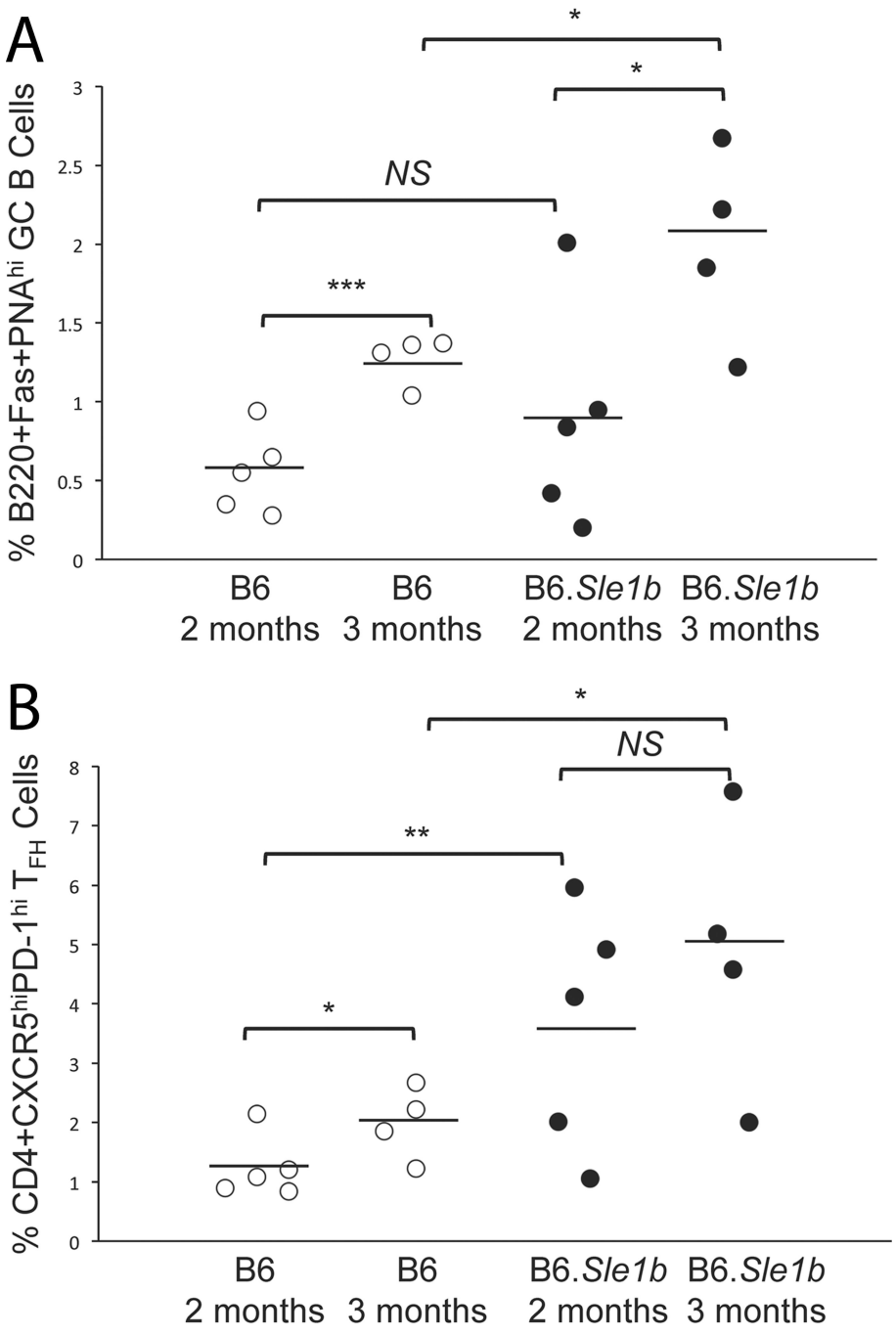

Figure 4. Sle1b induces spontaneous GC and T_{FH} cell responses at early age

Flow cytometric analysis of splenocytes obtained from 2 and 3 months old female B6 and B6.*Sle1b* mice for the percentages of GC B cells (A) and T_{FH} cells (B). The open circles represent B6 mice while the closed circles represent B6.*Sle1b* mice. Each circle represents an individual mouse and horizontal bars represent the mean values. Statistical analysis was performed as described in Materials and Methods.

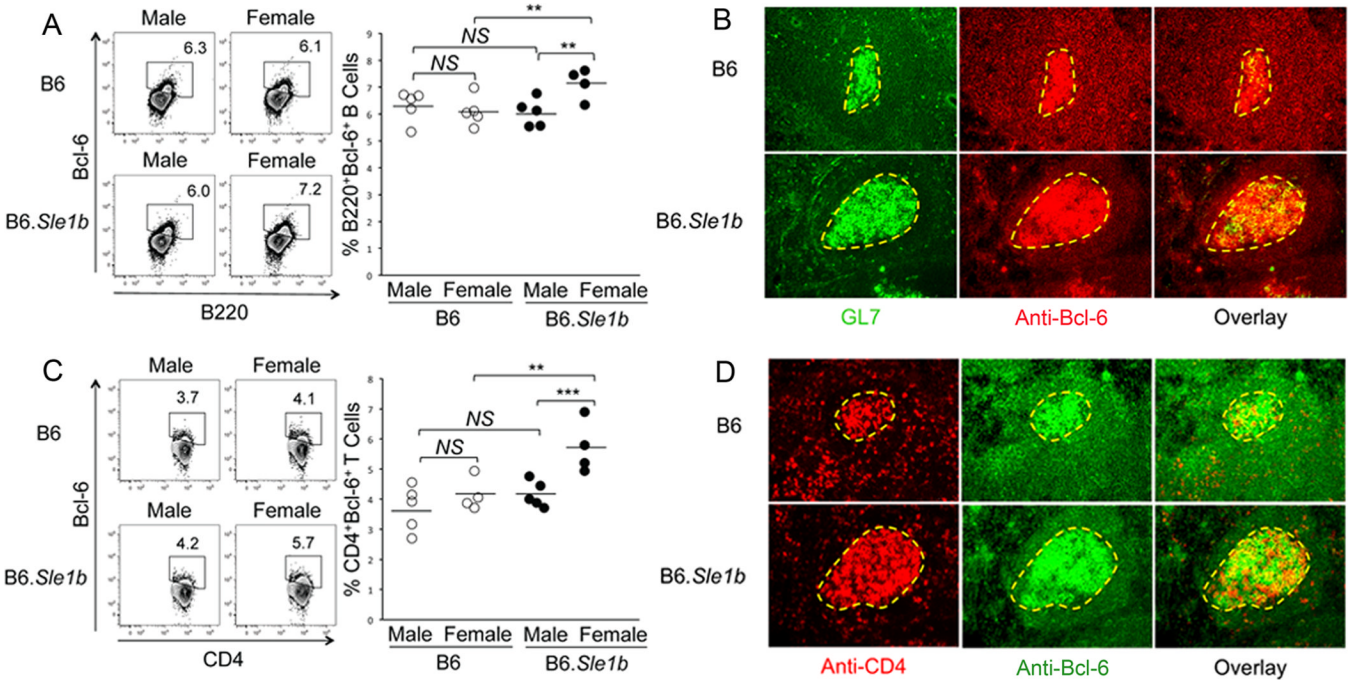

Figure 5. Increased number of Bcl-6 expressing B and CD4 T cells in B6.Sle1b female mice

Splenocytes obtained from sex matched, 6–9 month old B6 and B6.*Sle1b* mice were stained for Abs against either B220 and Bcl-6 (A) or CD4 and Bcl-6 (C) and analyzed by flow cytometry. The left flow cytometry plots are representative images from each group while the scatter plots on the right indicate the range of $B220^{+}Bcl\text{-}6^{+}$ B cell (A) and $CD4^{+}Bcl\text{-}6^{+}$ T cell (C) percentages from each group. Each circle represents an individual mouse and horizontal bars represent the mean values. Statistical analysis was performed as described in Materials and Methods. Spleen sections obtained from 6–9 month old female B6 and B6.*Sle1b* mice were either stained with GL7 (green) and anti-Bcl-6 (red) (B) or anti-CD4 (red) and anti-Bcl-6 (green) (D). The data shown in B and D were obtained from 4 to 5 female mice of each genotype. Original magnification of the images was 200×.

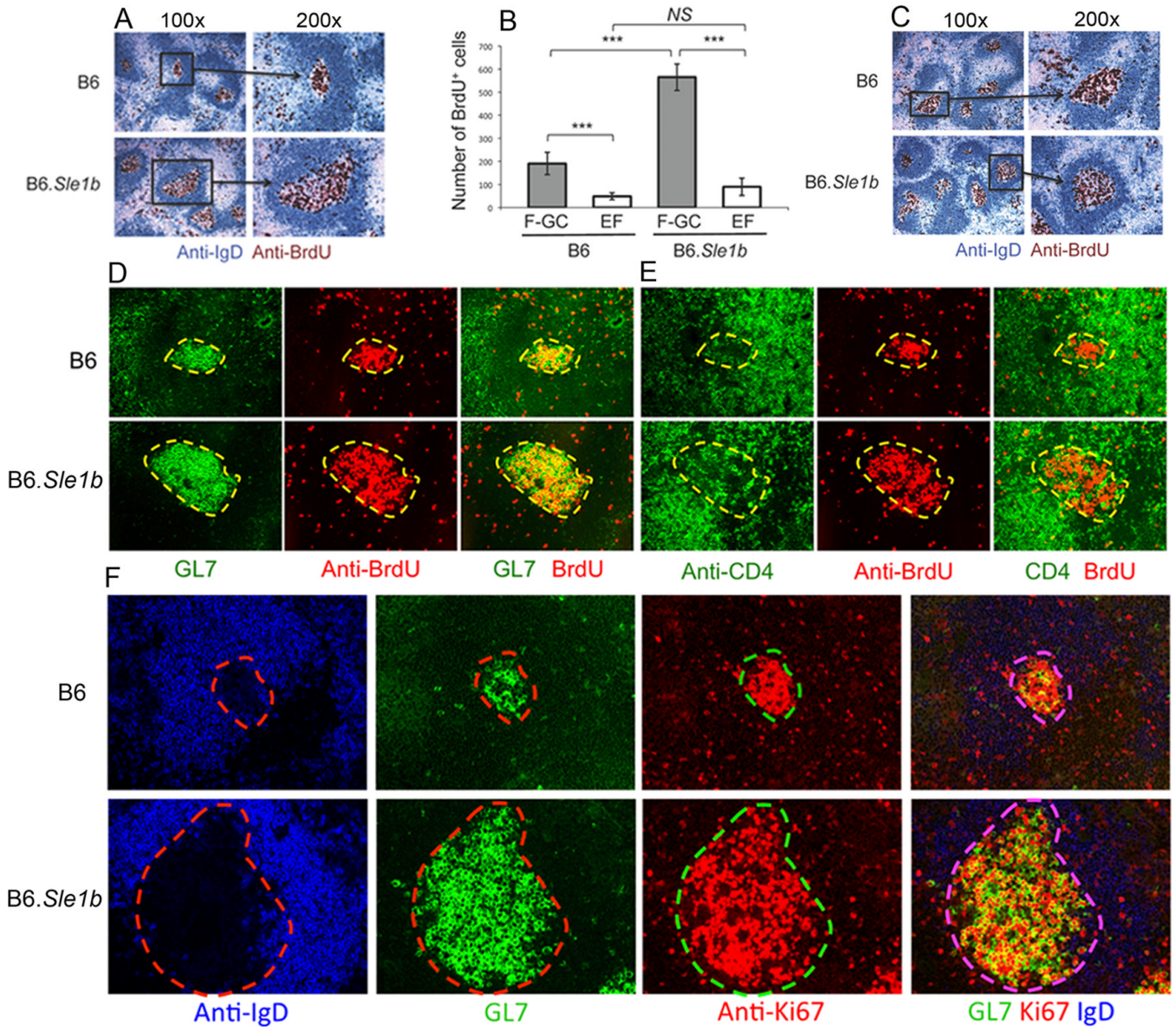

Figure 6. Significantly higher number of proliferating B cells in B6.Sle1b female mice

(A) Spleen sections from 6–9 month old B6 and B6.*Sle1b* mice injected with BrdU 12 hours and 1–2 hours prior to sacrifice were stained for anti-IgD (blue) and anti-BrdU (brown). Original magnification of the images was 100× (left) and 200× (right). (B) Semi-quantitative analysis of the number of $BrdU^+$ cells in follicular-GC (F-GC, gray bars) versus extrafollicular (EF, white bars) regions. $BrdU^+$ cells were counted in two randomly picked areas per spleen at ×100 original magnification. Five B6 and 5 B6.*Sle1b* female mice were analyzed. (C) Spleen sections obtained from SRBC-immunized 5–6 week old female B6 and B6.*Sle1b* mice were analyzed for $BrdU^+$ cells inside the GCs as described in A. Parallel spleen sections were obtained from 6–9 month old female B6 and B6.*Sle1b* mice and stained for either GL7 (green) and anti-BrdU (red) as shown in (D) or anti-CD4 (green) and anti-BrdU (red) as shown in (E). (F) Spleen sections from 6–9 month old female B6 and B6.*Sle1b* mice were stained for anti-IgD (blue), GL7 (green), and anti-Ki67 (red). Original magnification of the images in C-E was 200×. These data were generated from at least 5 female mice of each genotype.

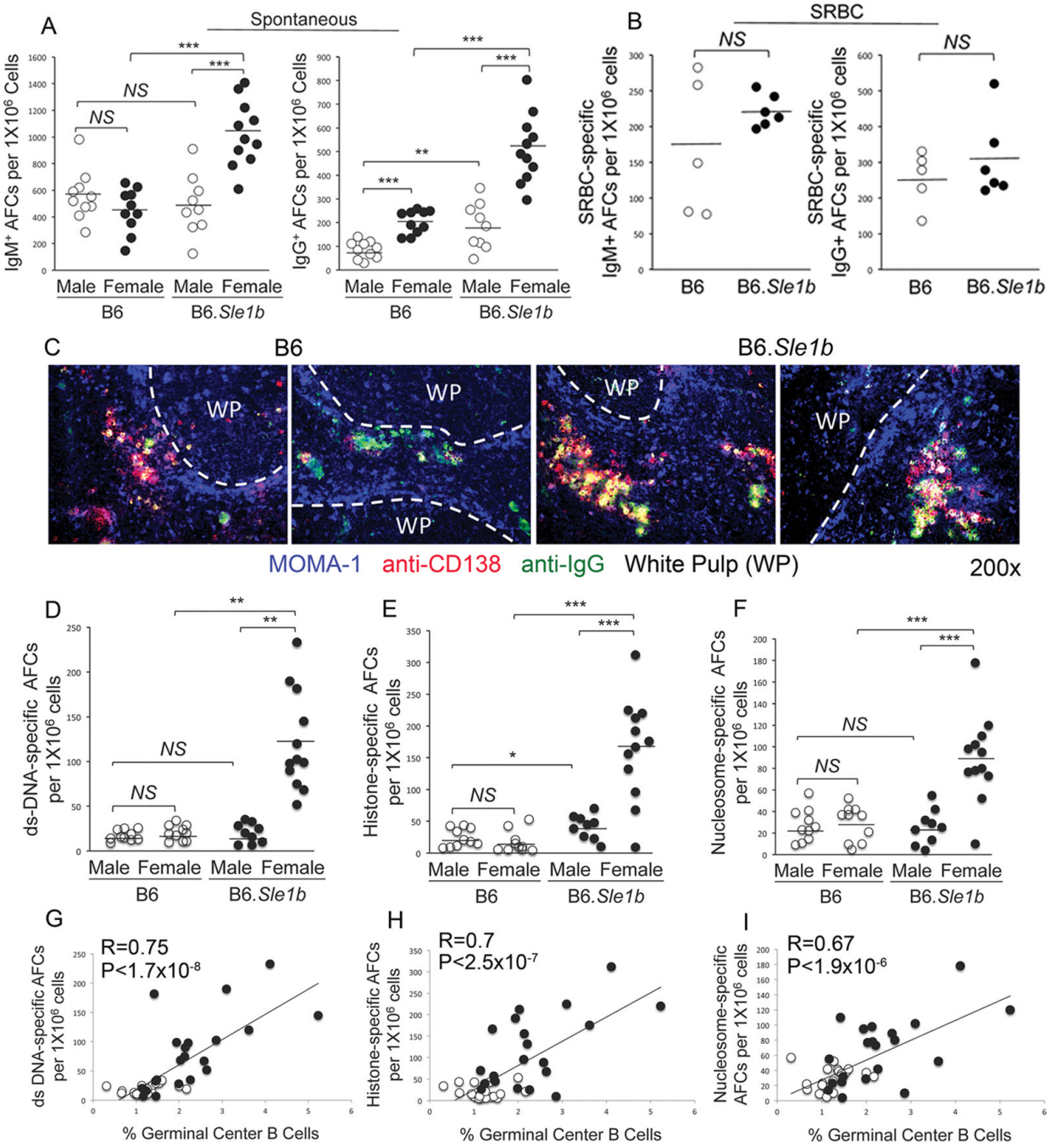

Figure 7. Increased ANA-specific AFCs in B6.Sle1b female mice

Total number of IgM (left panel) and IgG (right panel) specific AFCs in un-immunized 6–9 month old (A) and SRBC-immunized 5–6 week old (B), sex-matched B6 and B6.*Sle1b* mice were measured by ELISpot assay. (C) Spleen sections obtained from 6–9 month old female B6 and B6.*Sle1b* mice were stained for MOMA-1 (blue), anti-CD138 (red), and anti-IgG (green). WP represents white pulp. Original magnification of the images was 200x. Representative data from 5 female mice of each genotype are shown. The number of ds-DNA- (D), histone- (E), and nucleosome- (F) specific AFCs were measured by ELISpot assay. The degree of correlation between GC B cells and ds-DNA- (G), histone- (H), and nucleosome- (I) specific AFCs was analyzed. Each circle represents an individual mouse

and B6.*Sle1b* mice are depicted in black circles while B6 mice are depicted in white circles. Statistical analysis was performed as described in Materials and Methods.

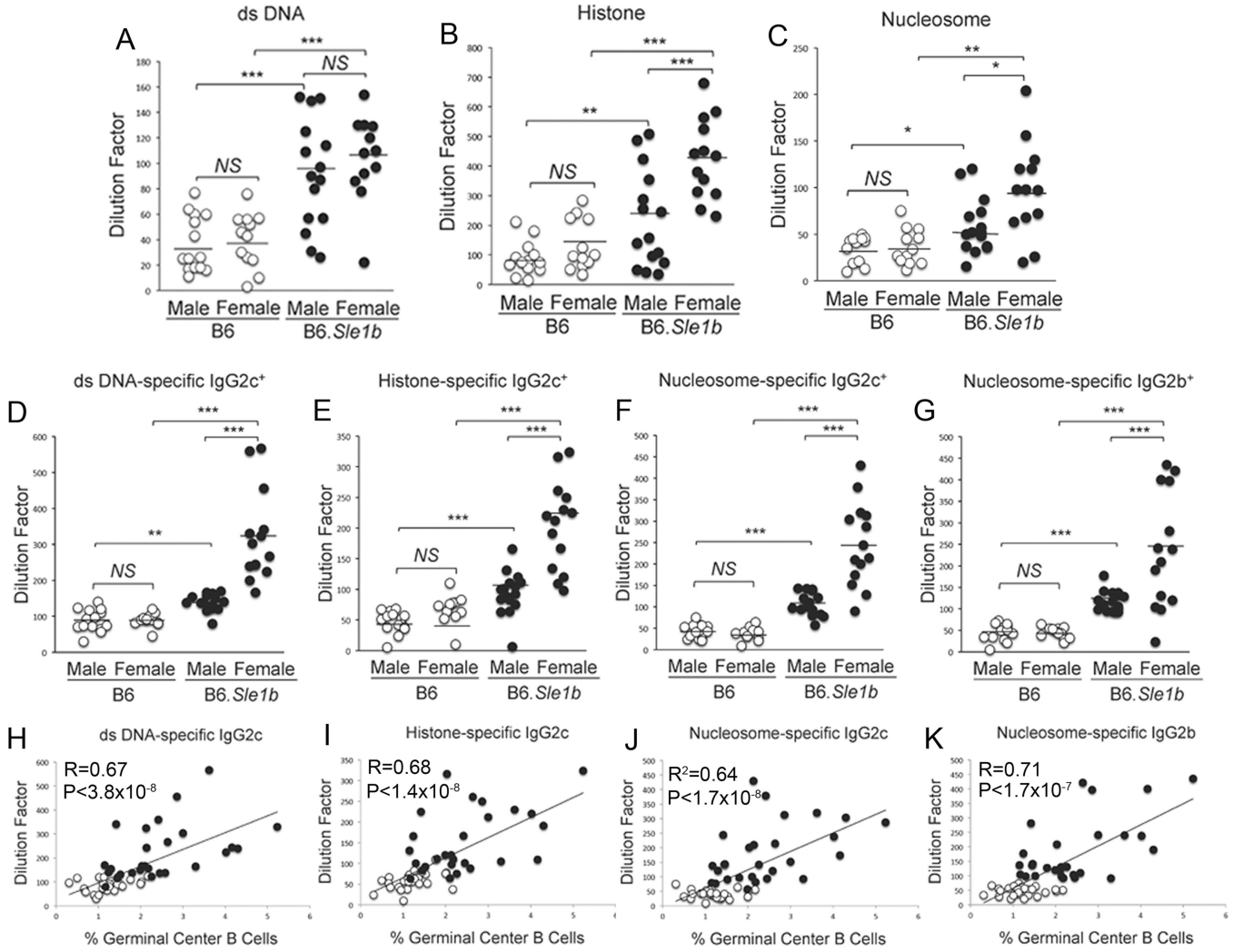

Figure 8. Elevated ANA-specific AFCs in female B6.Sle1b mice correlated with increased ANA-specific Ab titers

Total double-stranded DNA- (A), histone- (B), and nucleosome- (C) specific serum Ab titers were measured by ELISA in 6–9 month old, sex matched B6 and B6.*Sle1b* mice. Similarly, ds-DNA-(D), histone- (E) and nuclesosome (F and G)-reactive and IgG subclass-IgG2c/2b-specific ANA titers were measured in mice described in (A–C). Only the ANA-specific IgG subclasses that had elevated levels of Ab titers above baseline are shown. The degree of correlation between the percentage of Spt-GC B cells and IgG2c-2b specific and double-stranded DNA- (H), histone- (I), and nucleosome- (J–K) reactive serum Ab titers in 6–9 month old, sex matched B6 and B6.*Sle1b* mice are shown. Each circle represents an individual mouse and B6.*Sle1b* mice are depicted in black circles while B6 mice are depicted in white circles. Statistical analysis was performed as described in Materials and Methods.

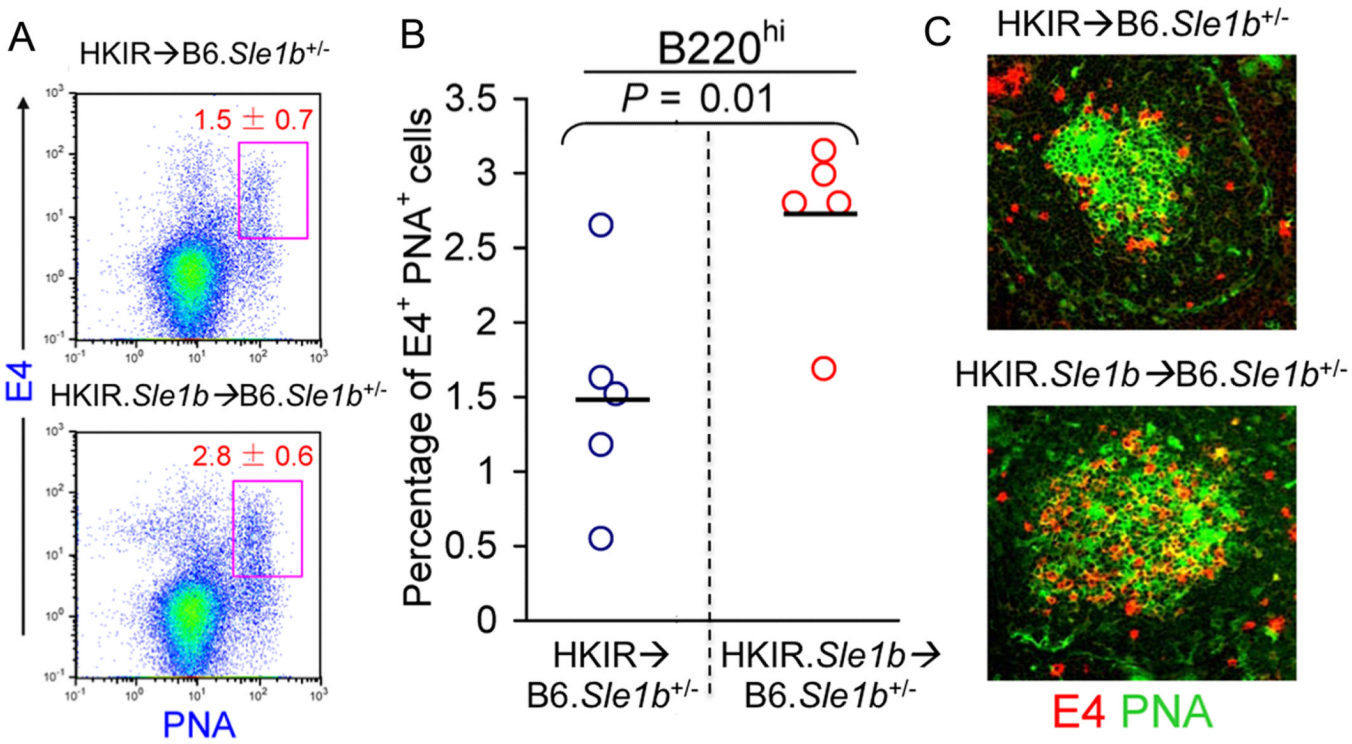

Figure 9. Augmented GC response of Ars-DNA dual-reactive HKIR B cells in the presence of Sle1b

Flow cytometric analysis was performed on splenocytes isolated from B6.*Sle1b*$^{+/-}$ mice receiving 2×10^6 HKIR or HKIR.*Sle1b* B cells and stained with the anti-idiotypic mAb E4 in combination with GC B cell markers B220 and PNA. The percentage of B220^{hi}E4^{+}PNA^{+} Ars-DNA dual reactive B cells in HKIR→ B6.*Sle1b*$^{+/-}$ and HKIR.*Sle1b* → B6.*Sle1b*$^{+/-}$ GCs is shown in rectangular gates (A) and in scatter plots (B). Each circle represents an individual mouse and horizontal bars represent the mean values. (C) Spleen sections from HKIR→ B6.*Sle1b*$^{+/-}$ (upper panel) and HKIR.*Sle1b* → B6.*Sle1b*$^{+/-}$ (lower panel) recipient mice were stained for E4 (red) and PNA (green). High magnification (200×) representative images from 5 mice of each genotype are displayed.

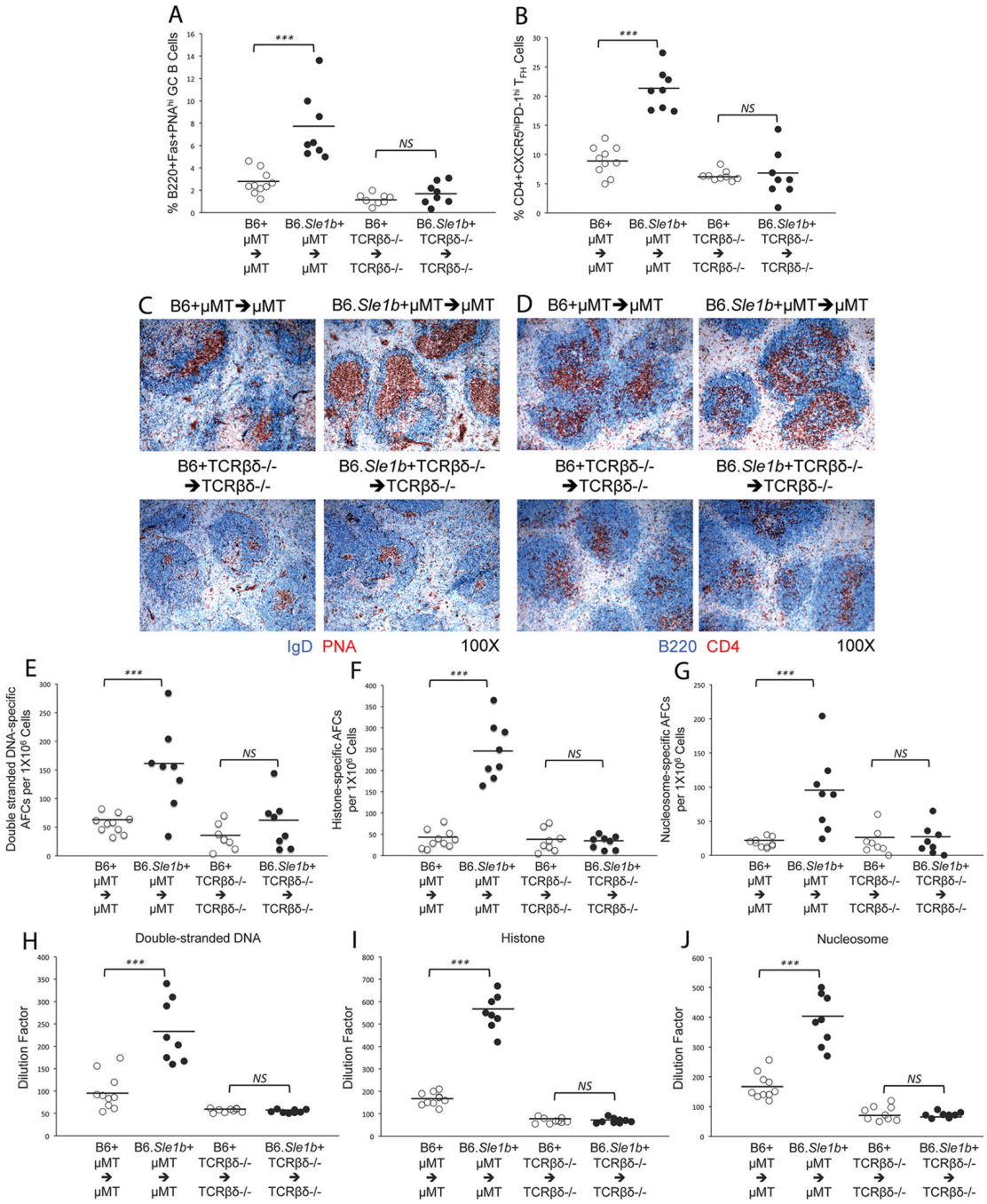

Figure 10. The Sle1b sub-locus primarily affects on B cells

Flow cytometric analysis was performed to evaluate the percentages of $B220^{+}Fas^{+}PNA^{hi}$ GC B cells (A) and $CD4^{+}CXCR5^{hi}PD\text{-}1^{hi}$ T_{FH} cells (B) in splenocytes obtained from B6 + μMT → μMT, B6.*Sle1b* + μMT → μMT, B6 + $TCR\beta\delta^{-/-}$ → $TCR\beta\delta^{-/-}$ and B6.*Sle1b* + $TCR\beta\delta^{-/-}$ → $TCR\beta\delta^{-/-}$ chimeras. Spleen sections from these mice were stained for either IgD (blue) and PNA (red) (C) or B220 (blue) and CD4 (red) (D). Original magnification of the images was 100x. The number of ds-DNA- (E), histone- (F), and nucleosome- (G) specific AFCs were measured by ELISpot assay. Total IgG ds-DNA- (H), histone- (I), and nucleosome- (J) specific ANA titers were measured by ELISA. The open circles represent B6 mice while the closed circles represent B6.*Sle1b* mice. Each circle represents an

individual mouse and horizontal bars represent the mean values. Statistical analysis was performed as described in Materials and Methods.